Published for SISSA by Springer

Received: *August 2, 2023*
Revised: *November 13, 2023*
Accepted: *December 12, 2023*
Published: *December 28, 2023*

Exploring slicing variables for jet processes

Luca Buonocore, Massimiliano Grazzini, Jürg Haag, Luca Rottoli and Chiara Savoini

Physik Institut, Universität Zürich,
CH-8057 Zürich, Switzerland

E-mail: lbuono@physik.uzh.ch, grazzini@physik.uzh.ch, juerg.haag@physik.uzh.ch, luca.rottoli@physik.uzh.ch, csavoi@physik.uzh.ch

Abstract: We consider the class of inclusive hadron collider processes in which one or more energetic jets are produced, possibly accompanied by colourless particles. We provide a general formulation of a slicing scheme for this class of processes, by identifying the various contributions that need to be computed up to next-to-leading order (NLO) in QCD perturbation theory. We focus on two novel observables, the one-jet resolution variable ΔE_t and the n-jet resolution variable k_T^{ness}, and explicitly compute all the ingredients needed to carry out NLO computations using these variables. We contrast the behaviour of these variables when the slicing parameter becomes small. In the case of k_T^{ness} we also present results for the hadroproduction of multiple jets.

Keywords: Higher-Order Perturbative Calculations, Jets and Jet Substructure

ArXiv ePrint: 2307.11570

https://doi.org/10.1007/JHEP12(2023)193

Contents

1 Introduction

Processes featuring multiple jets play a crucial role at hadron colliders. Many important new-physics signatures are characterised by multijet final states plus additional colourless particles. The evaluation of the corresponding cross sections and kinematical distributions in perturbative QCD requires the availability of the corresponding scattering amplitudes, and efficient methods to handle and cancel the associated infrared (IR) singularities. The required

JHEP12(2023)193

scattering amplitudes at tree level and one-loop can nowadays be obtained with automated tools, while two-loop amplitudes are available only for relatively simple processes (see e.g. refs. [1, 2] and references therein). Several methods to handle and cancel IR singularities have been developed and used to obtain perturbative QCD predictions at the next-to-next-to-leading order (NNLO) for many benchmark processes (see e.g. ref. [3]). Despite this, the availability and reproducibility of differential NNLO predictions by using public numerical programs is still limited to relatively simple processes [4–9].

Non-local subtraction or *slicing*[1] methods [14, 15] have provided very efficient ways to obtain NNLO predictions for a number of benchmark hadron collider processes involving colourless final states [16–37], possibly accompanied by one jet [38–41], and/or a heavy-quark pair [7, 42–46]. For the simplest processes even next-to-next-to-next-to leading order (N^3LO) results have been obtained [47–52] with such methods.

Slicing methods are based on identifying a resolution variable to distinguish configurations in which one or more additional QCD partons are resolved. The resolution variable is then used to introduce a cut in the phase space: the contribution below the cut can be approximated by exploiting the knowledge of the IR behaviour of the corresponding QCD matrix elements, while the contribution above the cut necessarily involves at least one additional parton and can be evaluated by performing a lower order computation. In the case of the production of a colourless final state and/or heavy quarks a well established resolution variable is the transverse momentum q_T of the triggered final state. In the case of multijet production a well-known resolution variable is N-jettiness [15], τ_N, which is defined on events containing at least N hard jets. Requiring $\tau_N \ll 1$ effectively provides an inclusive way to veto additional jets. Besides their applications as slicing variables, both q_T and N-jettiness have also been used as resolution variables in matching NNLO calculations to Monte Carlo parton showers [53–57]. Further examples of resolution variables in hadron collisions are provided by *shape variables* [58, 59], which are designed to measure the deviation from the leading order (LO) energy flow.

The advantage of slicing methods is in the fact that the cross section above the cut can be carried out in a simple way, and at NNLO it is obtained through well established local NLO subtraction schemes [60–64]. The price to pay is that the approximation of the cross section below the cut introduces a dependence on the slicing parameter. This dependence leads to missing power suppressed contributions and the exact result can be recovered only through a suitable extrapolation procedure.

There are several features that characterise a resolution variable. The process (in)dependence, the factorisation properties in the IR limit (and the related possibility to carry out all-order resummation), the absence of non-global logarithmic contributions [65], the qualitative behaviour and the quantitative impact of the power suppressed contributions are all important aspects to establish the extent to which a resolution variable can be useful. These aspects are in turn relevant also when the variable is used in the matching of fixed-order calculations to Monte Carlo parton showers. Therefore, the exploration of new resolution variables is interesting by itself, both in the context of fixed-order calculations

[1] The slicing method was introduced in the context of NLO calculations, first for e^+e^- annihilation [10–12] and, later, for hadron collisions [13].

JHEP12(2023)193

and of Monte Carlo generators.

In this paper we consider a rather general class of processes: the hadronic production of an arbitrary number of jets, possibly accompanied by a colourless system F. We start by providing a general formulation of a slicing scheme for this class of processes, by identifying the various contributions that need to be computed at NLO. These contributions correspond to what in Soft Collinear Effective Field Theory (SCET) [66–70] are called parton level *beam*, *jet* and *soft* functions. We then focus on two novel observables, the one-jet resolution variable ΔE_t and the n-jet resolution variable k_T^{ness} [71], and explicitly evaluate all the contributions necessary to implement an NLO computation by using these variables. We also present numerical results by contrasting the different power suppressed contributions affecting the two variables.

The paper is organised as follows. In section 2 we discuss the general structure of the NLO computation for an arbitrary resolution variable. In section 3 we consider two specific examples: in 3.1 we focus on the one-jet resolution ΔE_t variable for the $F+$jet process, while in section 3.2 we move to the k_T^{ness} variable. Our numerical results are presented in section 3.3. More details on the computations and analytical results are presented in the appendices.

2 Slicing at NLO for jet processes

2.1 Generalities

In this work we consider processes in which n hard jets are produced, possibly in association with a colourless system F. At the Born level, the kinematics of this process is fully determined by the momentum of the colourless system p_F and the momenta $p_1, p_2, p_3, \dots, p_{n+2}$ of $n+2$ hard QCD massless partons

$$a_1(p_1) + a_2(p_2) \to a_3(p_3) + \cdots + a_{n+2}(p_{n+2}) + F(p_F)\,, \tag{2.1}$$

where a_1, a_2,..., a_{n+2} denote the parton flavours. Momentum conservation implies

$$p_1 + p_2 = p_3 + \dots p_{n+2} + p_F \equiv q. \tag{2.2}$$

At NLO, we also have to consider real configurations with an additional unresolved parton with momentum k. In our notation, momenta labeled with Greek indices $\alpha = 1, 2 \dots n+2$ refer to all coloured massless Born level partons, while momenta labeled with Latin indices $i = 3 \dots n+2$ are associated with final-state partons. Concerning the flavour of a given QCD parton, we introduce a calligraphic capital letter $\mathcal{A}$ to define a multiindex describing a certain Born channel. For instance $\mathcal{A} = \{a_\alpha\} = \{a_1, a_2, \{a_i\}\}$ would refer to the channel $a_1 + a_2 \to \{a_i\} + F$.

At NLO, a slicing method based on a resolution variable r (that we assume to be properly normalised to make it dimensionless) is in general built by splitting the hadronic cross section into a contribution above and a contribution below a small cut r_{cut}

$$\begin{aligned}\sigma^{\text{NLO}} &= \int_{n+1} d\sigma^R + \int_n (d\sigma^V + d\sigma^B) \\ &= \int_{n+1} d\sigma^R \Theta(r - r_{\text{cut}}) + \left(\int_{n+1} d\sigma^R \Theta(r_{\text{cut}} - r) + \int_n (d\sigma^V + d\sigma^B) \right)\,,\end{aligned} \tag{2.3}$$

JHEP12(2023)193

where $d\sigma^B$and $d\sigma^R$ are the Born and real emission contributions respectively, while $d\sigma^V$ contains the genuine loop-tree interference diagrams and the mass factorisation counterterms

$$\int_n d\sigma^V = \mathcal{V} + \mathcal{C}_{\overline{\text{MS}}}\,. \tag{2.4}$$

The contribution above the cut is IR-finite in $d = 4$ dimensions and it can be integrated numerically with a Monte Carlo method. The calculation of the contribution below the cut can be carried out in an analytic fashion by approximating the phase space, the resolution variable and the real matrix element in the relevant IR limits. The integration needs to be performed in $d = 4 - 2\epsilon$ dimensions and the IR poles from the real integration cancel the explicit poles from $d\sigma^V$. Throughout this paper we work in the conventional dimensional regularisation (CDR) scheme, with two polarisations for massless (anti-)quarks and $d-2$ polarisations for gluons. The strong coupling $\alpha_S(\mu_R)$ is renormalised in the $\overline{\text{MS}}$-scheme and related to the bare coupling α_S^u via

$$\alpha_S^u \mu_0^{2\epsilon} S_\epsilon = \alpha_S(\mu_R)\mu_R^{2\epsilon}\left[1 - \frac{\alpha_S(\mu_R)}{\pi}\frac{\beta_0}{\epsilon} + \mathcal{O}(\alpha_S^2)\right], \tag{2.5}$$

where $S_\epsilon = (4\pi)^\epsilon e^{-\gamma_E \epsilon}$, $\beta_0 = 11C_A/12 - T_R n_f/3$ and μ_R is the renormalisation scale. The SU(N_c) QCD colour factors are $C_F = (N_c^2-1)/(2N_c)$, $C_A = N_c$, $T_R = 1/2$ and n_f is the number of massless flavours. In general we can write the contribution below the cut as

$$\begin{aligned}
&\int_{n+1} d\sigma^R \Theta(r_{\text{cut}} - r) + \int_n (d\sigma^V + d\sigma^B) \\
&= \sum_{\mathcal{A},\{b_1,b_2\}} \int_0^1 dx_1 \int_0^1 dx_2 \int_{x_1}^1 \frac{dz_1}{z_1} \int_{x_2}^1 \frac{dz_2}{z_2} f_{b_1}\left(\frac{x_1}{z_1}, \mu_F\right) f_{b_2}\left(\frac{x_2}{z_2}, \mu_F\right) \\
&\quad \times \int \frac{d\Phi_B}{2Q^2} \langle \mathcal{M}_{\mathcal{A}}^{(0)}| \left[\mathbf{\Sigma}^{00}_{\mathcal{A}b_1b_2}(z_1,z_2) + \frac{\alpha_S(\mu_R)}{\pi}\left(\sum_{k=0}^{2} \mathbf{\Sigma}^{1k}_{\mathcal{A}b_1b_2}(z_1,z_2)\log^k(r_{\text{cut}}) + \mathcal{O}(r_{\text{cut}}^p)\right)\right] |\mathcal{M}_{\mathcal{A}}^{(0)}\rangle\,,
\end{aligned} \tag{2.6}$$

where $d\Phi_B$ is the four-dimensional Born phase space, $Q = \sqrt{q^2}$ is the invariant mass of the Born event and $|\mathcal{M}_{\mathcal{A}}^{(0)}\rangle$ is the Born matrix element (which can be evaluated here in $d = 4$ dimensions), with $|\cdot\rangle$ denoting a vector in colour space (see e.g. ref. [61]). In the above formula, $f_a(x, \mu_F)$ is the parton distribution function (PDF) of parton a carrying a fraction x of the proton momentum at the factorisation scale μ_F. Bold symbols denote operators acting on colour space and we defined

$$\mathbf{\Sigma}^{00}_{\mathcal{A}b_1b_2}(z_1,z_2) = \mathbf{1}\delta_{a_1b_1}\delta_{a_2b_2}\delta(1-z_1)\delta(1-z_2)\,, \tag{2.7}$$

where $\mathbf{1}$ is the identity operator in colour space. We anticipate that in eq. (2.6) the missing power corrections in r_{cut} can be logarithmically enhanced for some slicing variables.

The complicated part of the calculation is the integration of the real emission contribution over the 1-particle radiation phase space subjected to the constraint $r < r_{\text{cut}}$, retaining the full dependence on the Born kinematics. Indeed, in this region, the integral is dominated by configurations in which a parton is soft and/or is radiated collinearly to one of the $n+2$

JHEP12(2023)193

external legs. In order to extract the leading power behaviour in $r_{\rm cut}$, our strategy is based on approximating both the real matrix element squared, using the factorisation properties of QCD tree-level amplitudes, and the observable r in the relevant IR limits. The treatment of the phase space requires some care. Indeed, a naive approximation of the phase space in the different limits may lead to integrals that are divergent in d dimensions. This is the well-known problem of rapidity divergences [72–74] occurring in approaches based on the method of regions [75, 76], such as SCET.

In the following we will detail the construction of suitable approximations to obtain the analytic expression, at leading power, for the real emission contribution below the cut. To achieve this result, it is natural to organise the calculation by separating the IR singular regions as

$$\int_{n+1} d\sigma^R \Theta(r_{\rm cut} - r) = \mathcal{I}^c + \mathcal{F}^c + \mathcal{S}^{wa}\,, \tag{2.8}$$

i.e. as a sum of initial-state collinear contributions, $\mathcal{I}^c$, final-state collinear contributions, $\mathcal{F}^c$, and a soft one, $\mathcal{S}^{wa}$. These three quantities must be properly defined to avoid the double counting in the soft-collinear regions. In our approach, we retain the relevant soft-collinear configurations in $\mathcal{I}^c$ and $\mathcal{F}^c$ and include the left-over soft wide-angle emissions in $\mathcal{S}^{wa}$, thus avoiding double counting. The resulting ingredients lead to the definition of perturbative beam, jet and soft functions, following the nomenclature used in the SCET literature.[2]

2.2 Initial-state collinear limit

In this section we outline the computation of the initial-state collinear contribution in the region below the cut, $r < r_{\rm cut}$,

$$\mathcal{I}^c \equiv \mathcal{I}^c_1 + \mathcal{I}^c_2 = \int_{n+1} \left(d\sigma_{\mathcal{I}^c_1} \Theta(r_{\rm cut} - r^{\mathcal{I}^c_1}) + d\sigma_{\mathcal{I}^c_2} \Theta(r_{\rm cut} - r^{\mathcal{I}^c_2}) \right), \tag{2.9}$$

where $r^{\mathcal{I}^c_1}$ and $r^{\mathcal{I}^c_2}$ are approximations of the resolution variable in the limit where the radiated parton with momentum k becomes collinear to the initial-state parton p_1 and p_2, respectively. The differential cross section $d\sigma_{\mathcal{I}^c_i}$ includes the real phase space $d\Pi_R(\{p_j\}, k)$, the real matrix element in the collinear limit $k \cdot p_i \to 0$ and the convolution with the PDFs. In the following, we will provide a proper parametrisation for the real phase space $d\Pi_R(\{p_j\}, k)$ in the initial-state collinear limit.

Without loss of generality, we focus on the collinear limit $k \cdot p_1 \to 0$. We start from the expression of the real-emission phase space in $d = 4 - 2\epsilon$ dimensions

$$d\Pi_R(\{p_j\}, k) = [dk] \prod_{i=3}^{n+2} [dp_i]\, [dp_F]\, (2\pi)^d \delta^{(d)} \left(p_1 + p_2 - k - \sum_{i=3}^{n+2} p_i - p_F \right), \tag{2.10}$$

where we have used the short hand notation $[dp]$ for the 1-particle phase space element

$$[dp] \equiv \frac{d^d p}{(2\pi)^{d-1}} \delta^+(p^2 - m^2)\,. \tag{2.11}$$

[2] Notice that our definitions may differ from those customarily used in SCET. See appendix D for further details on the comparison between the SCET jet function and the one defined in this work.

JHEP12(2023)193

We introduce the four-momentum $q^\mu = p_1^\mu + p_2^\mu - k^\mu = p_F^\mu + \sum_{i=3}^{n+2} p_i^\mu$ of all final-state particles but the radiated parton, and we rewrite $d\Pi_R(\{p_j\}, k)$ as

$$\begin{aligned} d\Pi_R(\{p_j\}, k) &= [dk]\, d^d q\, \delta^{(d)}(p_1 + p_2 - k - q) \prod_{i=3}^{n+2} [dp_i]\, [dp_F]\, (2\pi)^d \delta^{(d)} \left(q - \sum_{i=3}^{n+2} p_i - p_F \right) \\ &= d^d q\, [dk]\, \delta^{(d)}(p_1 + p_2 - k - q) d\Pi_n^d(q; p_F, \{p_i\})\,, \end{aligned} \tag{2.12}$$

where $d\Pi_n^d(q; p_F, \{p_i\})$ is the d-dimensional Lorentz-invariant phase space for a particle of four-momentum q splitting into n partons $\{p_i\}_{i=3,\dots,n+2}$ plus a colourless system p_F. It is worth mentioning that the four-momentum q has a non-zero transverse component with respect to the direction of the colliding protons.

The radiation phase space $[dk]$ can be parametrised as

$$[dk] = \frac{1}{4(2\pi)^{3-2\epsilon}} (k_t^2)^{-\epsilon} dk_t^2 \frac{d\cos\theta}{1 - \cos^2\theta}\, d\Omega_{2-2\epsilon}\,, \tag{2.13}$$

where θ is the polar angle with respect to the beam axis in the partonic centre-of-mass (CM) frame, $k_t = k^0 \sin\theta$ is the transverse momentum of the radiation and $d\Omega_{2-2\epsilon}$ spans the directions in the $(2-2\epsilon)$-dimensional transverse space. Performing a change of variables, we can write the radiation phase space as

$$[dk] = \frac{1}{4} (k_t^2)^{-\epsilon}\, dk_t^2 \frac{dz}{\sqrt{(1-z)^2 - 4z k_t^2/Q^2}} \frac{d\Omega_{2-2\epsilon}}{(2\pi)^{3-2\epsilon}}\,, \tag{2.14}$$

where we defined $Q = \sqrt{q^2}$ and the energy fraction $z = \frac{Q^2}{\hat{s}}$, at fixed $\hat{s} = (p_1 + p_2)^2$.

Since we are interested in the radiation collinear to p_1, we can approximate k with $(1-z)p_1$ in the argument of the delta-function in eq. (2.12), dropping power suppressed contributions in k_t. The final expression for the real-emission phase space valid at leading power is

$$d\Pi_R(\{p_j\}, k) = \frac{(4\pi^2)^\epsilon}{32\pi^3}\, d\Omega_{2-2\epsilon} \frac{dk_t^2}{(k_t)^{2\epsilon}} \frac{dz}{\sqrt{(1-z)^2 - 4z k_t^2/Q^2}}\, d\Pi_n^d(q; p_F, \{p_i\}_{i=3}^{n+2})\,. \tag{2.15}$$

The matrix element squared for the real emission process $b_1 + b_2 \to b + \{a_i\} + F$ is denoted as $|\mathcal{M}_{b_1 b_2; b\{a_i\}}|^2$, and in the collinear limit it assumes the well-known form

$$|\mathcal{M}_{b_1 b_2; b\{a_i\}}|^2 \approx \frac{8\pi\alpha_S^u \mu_0^{2\epsilon}}{z p_1 \cdot k} \hat{P}_{a_1 b_1}^{s s'}(z, \hat{k}_t; \epsilon) \mathcal{T}_{a_1 b_2; \{a_i\}}^{s s'}. \tag{2.16}$$

In eq. (2.16) the squared matrix element is implicitly assumed to be averaged (summed) over the colours and polarisations of the initial (final) state partons. Unless stated otherwise, we shall use the same convention for all the squared matrix elements appearing in the paper. The ϵ dependence of the matrix elements is always understood. For a given Born matrix element

$$\mathcal{M}_{\mathcal{A}}^{c_1, c_2, \dots; s_1, s_2, \dots}(p_1, p_2, \dots)\,, \tag{2.17}$$

where $\{c_1, c_2, \dots\}$ and $\{s_1, s_2, \dots\}$ denote colour and spin indices respectively, we defined the spin polarisation tensor

$$\begin{aligned} &\mathcal{T}_{\mathcal{A}}^{s_\alpha s'_\alpha}(p_1, \dots, p_\alpha, \dots) \\ &\equiv \frac{1}{\mathcal{S}} \sum_{\text{spins}\, \neq s_\alpha, s'_\alpha} \overline{\sum_{\text{colours}}}\, \mathcal{M}_{\mathcal{A}}^{c_1, c_2, \dots; s_1, \dots s_\alpha \dots}(p_1, p_2, \dots) \left[\mathcal{M}_{\mathcal{A}}^{c_1, c_2, \dots; s_1, \dots s'_\alpha \dots}(p_1, p_2, \dots) \right]^\dagger, \end{aligned} \tag{2.18}$$

JHEP12(2023)193

where $\overline{\sum}$ indicates an average (sum) over the spins and colours of initial (final) state partons. The spin of the parton with momentum p_α is not summed over. However, we include a factor $1/\mathcal{S}$, where $\mathcal{S}$ corresponds to the number of polarisations of the parton α if it is an initial-state parton and $\mathcal{S} = 1$ otherwise. The fermion spin indices are $s_\alpha = \pm 1$ while it is convenient to label the gluon spin s_α with the corresponding Lorentz index $\mu = 1, \dots, d$. In eq. (2.16) $\hat{P}^{ss'}_{a_1 b_1}$ is the unregularised Altarelli-Parisi splitting function for a splitting $b_1(p_1) \to a_1(zp_1) + b((1-z)p_1)$ defined in appendix B. The spin indices in the polarisation tensor defined in eq. (2.18) are those of the parton a_1 (i.e. the one that undergoes the collinear splitting).

We notice that the change of variable $\cos\theta \to z$ is not invertible for $\cos\theta \in [-1, 1]$, and, therefore, the integrand has to be evaluated separately for positive (forward) and negative (backward) values of $\cos\theta$. The radiation phase space element is the same in the two θ-integration regions since it is an even function of $\cos\theta$. Furthermore, in the collinear limit, we can always choose an approximation of the resolution variable that is forward-backward symmetric. Thus, the only contribution sensitive to the forward/backward direction is the collinear matrix element, and, more precisely, such a dependence is entirely due to the term $\frac{1}{p_1 \cdot k}$. Therefore, we can replace the latter term by the symmetric combination

$$\frac{1}{p_1^0 k^0}\left(\frac{1}{1-\cos\theta} + \frac{1}{1+\cos\theta}\right) = \frac{2(1-z)}{k_t^2}, \tag{2.19}$$

and consider only the integral in the interval $\cos\theta \in [0, 1]$. By combining the phase space parametrisation and the collinear approximation of the real matrix element for both initial-state collinear regions and summing over the Born channels, we derive the leading power contribution due to the initial-state collinear splittings as

$$\begin{aligned}\mathcal{I}^c = \sum_{\mathcal{A}} \sum_{\{b_1,b_2\}} \int_0^1 dx_1 \int_0^1 dx_2 \int \frac{d\Pi_n^d(q; p_F, \{p_i\}_{i=3}^{n+2})}{2Q^2} \\ \times \int_{x_1}^1 \frac{dz_1}{z_1} \int_{x_2}^1 \frac{dz_2}{z_2} \mathcal{I}^{b_1 b_2}_{a_1 a_2}(z_1, z_2) f_{b_1}(x_1/z_1, \mu_F) f_{b_2}(x_2/z_2, \mu_F)\,,\end{aligned} \tag{2.20}$$

where

$$\mathcal{I}^{b_1 b_2}_{a_1 a_2}(z_1, z_2) = \mathcal{T}^{ss'}_{a_1 b_2; \{a_i\}} \mathcal{B}^{ss'}_{a_1 b_1}(z_1, r_{\rm cut}) \delta(1-z_2) + \mathcal{T}^{ss'}_{b_1 a_2; \{a_i\}} \delta(1-z_1) \mathcal{B}^{ss'}_{a_2 b_2}(z_2, r_{\rm cut}) \tag{2.21}$$

is written in terms of the *cumulant* NLO beam function

$$\begin{aligned}\mathcal{B}^{ss'}_{ab}(z, r_{\rm cut}) = \left(\frac{\mu_R^2}{Q^2}\right)^\epsilon \frac{e^{\gamma_E \epsilon}}{\Gamma(1-\epsilon)} \frac{\alpha_{\rm S}(\mu_R)}{\pi} \\ \times \int_0^\infty \frac{dx^2}{(x^2)^{1+\epsilon}} \int \frac{d\Omega_{d-2}}{\Omega_{d-2}} \hat{P}^{ss'}_{ab}(z, \hat{k}_t; \epsilon) \frac{\Theta(1-2x-z)}{\sqrt{1-4x^2/(1-z)^2}} \Theta(r_{\rm cut} - r^{\mathcal{I}^c})\,.\end{aligned} \tag{2.22}$$

In the above formulæ we identified $Q^2 = x_1 x_2 s$ and we introduced the dimensionless variable $x^2 = k_t^2/Q^2$. In eq. (2.22), the upper limit in the integral over z, encoded in the theta function, comes from the small x expansion of the physical solution of the equation

JHEP12(2023)193

$1-4zx^2/(1-z)^2 \sim 1-4x^2/(1-z)^2 = 0$, associated with a vanishing argument of the square root appearing in the denominator, and it sets a kinematical endpoint $z < 1$ for soft emissions. We stress that, in a strict power counting in the pure collinear limit $x \to 0$, the square root factor appearing in eq. (2.22) could be approximated with 1 and, correspondingly, the upper limit in the z integration extended to 1. However, this procedure may lead to the appearance of rapidity divergences, depending on the specific observable under consideration. In particular, rapidity divergences appear for observables that behave as a transverse momentum in the collinear limit.[3] We observe that retaining this term is consistent with a power counting valid both in the soft and collinear limits, according to the homogeneous scaling $x \sim \lambda$ and $1-z \sim \lambda$ for a small parameter λ.

We can further manipulate eq. (2.22) under the assumption that, at fixed k_t, $r^{\mathcal{I}^c}$ is a regular function of z in the soft limit $z \to 1$, which is valid for observables that scale as a transverse momentum in the initial-state collinear limit.[4] Then, for such observables we safely approximate

$$\frac{\Theta(1-2x-z)}{\sqrt{1-4x^2/(1-z)^2}}\hat{P}_{ab}^{ss'}(z,\hat{k}_t;\epsilon) = P_{ab}^{ss'}(z,\hat{k}_t;\epsilon) + d_a^{ss'}\delta_{ab}\delta(1-z)(-\gamma_a - C_a\log(x)) + \mathcal{O}(x)\,, \tag{2.23}$$

where

$$d_a^{ss'} = \begin{cases} \delta^{ss'} & a = q,\bar{q} \\ -g^{\mu\nu} & a = g \end{cases} \tag{2.24}$$

and $P_{ab}^{ss'}$ are the regularised splitting kernels reported in appendix B. We use

$$C_a = \begin{cases} C_F & a = q,\bar{q} \\ C_A & a = g \end{cases} \tag{2.25}$$

and we define the coefficients

$$\gamma_q = \frac{3}{4}C_F\,, \qquad \gamma_g = \beta_0 = \frac{11}{12}C_A - \frac{1}{3}T_R n_f\,. \tag{2.26}$$

2.3 Final-state collinear limit

In this section we outline the computation of the final-state collinear contribution in the region below the cut, $r < r_{\text{cut}}$,

$$\mathcal{F}^c \equiv \sum_{i=3}^{n+2}\mathcal{F}_i^c = \sum_{i=3}^{n+2}\int_{n+1} d\sigma_{\mathcal{F}_i^c}\Theta(r_{\text{cut}} - r^{\mathcal{F}_i^c})\,, \tag{2.27}$$

where $r^{\mathcal{F}_i^c}$ refers to an approximation of the resolution variable in the limit where the radiated parton with momentum k becomes collinear to the final-state parton p_i. In eq. (2.27), the differential cross section $d\sigma_{\mathcal{F}_i^c}$ includes the real phase space $d\Pi_R(\{p_j\},k)$, the real matrix

[3] In SCET, the distinction is between SCET_I, which do not need a rapidity regulator, and SCET_II observables, which do need it.

[4] Notice that this is not the case for observables like N-jettiness that scales as $k_t^2/(Q^2(1-z))$.

JHEP12(2023)193

element in the collinear limit $k \cdot p_i \to 0$ and the convolution with the PDFs. For the sake of concreteness, we will focus on the region where k becomes collinear to the final-state coloured parton with momentum p_i. In the following, we parallel the discussion carried out for initial-state radiation. We start from a suitable approximation of the real phase space in the relevant collinear limit. We consider eq. (2.10) and we recast the phase space elements associated with the two collinear partons as

$$[dp_i][dk] = \frac{d^{d-1}\vec{p}_i}{(2\pi)^{d-1}2p_i^0}\frac{d^{d-1}\vec{k}}{(2\pi)^{d-1}2k^0} = \frac{d^{d-1}\vec{\tilde{p}}_i}{(2\pi)^{d-1}2\tilde{p}_i^0}\frac{\tilde{p}_i^0}{p_i^0}\frac{d^{d-1}\vec{k}}{(2\pi)^{d-1}2k^0} = [d\tilde{p}_i]\frac{\tilde{p}_i^0}{p_i^0}[dk] \tag{2.28}$$

with $\tilde{p}_i^\mu = (\tilde{p}_i^0, \vec{\tilde{p}}_i) = (p_i^0 + k^0, \vec{p}_i + \vec{k})$, from which it follows that the real phase space can be written as

$$d\Pi_R(\{p_j\}, k) = d\Pi_n^d(q; p_F, \{p_3, \dots, \tilde{p}_i, \dots, p_{n+2}\})\frac{\tilde{p}_i^0}{p_i^0}[dk]\,, \tag{2.29}$$

where $q = p_1 + p_2$. We parametrise the radiation phase space in spherical coordinates as

$$[dk] = \frac{1}{2(2\pi)^{3-2\epsilon}}(k^0)^{1-2\epsilon}\sin^{1-2\epsilon}\theta dk^0 d\theta d\Omega_{2-2\epsilon}\,, \tag{2.30}$$

where θ is the angle between $\vec{k}$ and $\vec{\tilde{p}}_i$. We reparametrise the phase space in terms of the energy fraction $\xi = k^0/\tilde{p}_i^0$ and the invariant mass $\tilde{s}_i = \tilde{p}_i^2$. Performing an expansion in small $\tilde{s}_i$ we obtain the following expression valid at leading power in the collinear limit

$$\frac{\tilde{p}_i^0}{p_i^0}[dk] = \frac{1}{4(2\pi)^{3-2\epsilon}}\,d\xi\xi^{-\epsilon}(1-\xi)^{-\epsilon}\,d\tilde{s}_i\tilde{s}_i^{-\epsilon}\left(1 - \frac{\tilde{s}_i(1-2\xi)^2}{4(\tilde{p}_i^0)^2\xi(1-\xi)}\right)^{-\epsilon} d\Omega_{2-2\epsilon}\,. \tag{2.31}$$

This result agrees with standard collinear parametrisations, see for example ref. [77], apart from the last factor in parenthesis. As discussed in the previous section, this factor allows us to retain some terms which contribute beyond the strict collinear limit but make the integral finite without the need of introducing additional regulators. In particular, we count $\tilde{s}_i/\left[(\tilde{p}_i^0)^2\xi\right] \sim 1$ ($\tilde{s}_i/\left[(\tilde{p}_i^0)^2(1-\xi)\right] \sim 1$), where $\xi \to 0$ ($\xi \to 1$) corresponds to parton k (p_i) becoming soft. Note that we can further approximate

$$\frac{\tilde{s}_i(1-2\xi)^2}{4(\tilde{p}_i^0)^2\xi(1-\xi)} \sim \frac{\tilde{s}_i}{4(\tilde{p}_i^0)^2\xi(1-\xi)}\,, \tag{2.32}$$

which is valid in both limits $\xi \to 0$ and $\xi \to 1$. The matrix element squared for the corresponding splitting process $a_i(\tilde{p}_i) \to a(k) + b(p_i)$ can be approximated in the collinear limit as

$$|\mathcal{M}_{a_1a_2;\dots a,b\dots}|^2 \approx \frac{8\pi\alpha_S^u\mu_0^{2\epsilon}}{k\cdot p_i}\hat{P}^{ss'}_{a_i\to ab}(\xi, \hat{k}_\perp; \epsilon)\mathcal{T}^{ss'}_{a_1a_2;\dots a_i\dots} \tag{2.33}$$

where $\hat{P}^{ss'}_{a_i\to ab}$ is the Altarelli-Parisi splitting function defined in appendix B and the spin-polarisation tensor $\mathcal{T}^{ss'}_{\mathcal{A}}$ is defined in eq. (2.18). In this case, the spin indices s, s' in the polarisation tensor are those of the parton a_i and $\hat{k}_\perp$ refers to the transverse momentum with respect to the direction of $\tilde{p}_i$. The full contribution $\mathcal{F}_i^c$, associated with the collinear

JHEP12(2023)193

limit $k \cdot p_i \to 0$, is obtained by summing over all Born channels $\mathcal{A} = \{a_1, a_2, \{a_i\}\}$ and over all possible splittings $a_i \to (*)$ of the parton a_i. Thus, we find that

$$\begin{aligned}\mathcal{F}_i^c = &\sum_{\mathcal{A}} \int_0^1 dx_1 f_{a_1}(x_1,\mu_F) \int_0^1 dx_2 f_{a_2}(x_2,\mu_F) \int d\Pi_n^d(q; p_F, \{p_3,\dots,\tilde{p}_i,\dots,p_{n+2}\}) \frac{\mathcal{T}^{ss'}_{a_1 a_2;\dots a_i\dots}}{2Q^2} \\ &\times \frac{\left(\frac{4\pi\mu_0^2}{Q^2}\right)^\epsilon}{\Gamma(1-\epsilon)} \frac{\alpha_{\rm S}^u}{\pi} \sum_{(*)} \int \frac{d\Omega_{d-2}}{\Omega_{d-2}} \int_0^1 d\xi \xi^{-\epsilon}(1-\xi)^{-\epsilon} \\ &\times \int_0^{4(\tilde{p}_i^0)^2/Q^2\xi(1-\xi)} d\tilde{x}_i \tilde{x}_i^{-1-\epsilon} \left(1 - \frac{Q^2}{4(\tilde{p}_i^0)^2} \frac{\tilde{x}_i}{\xi(1-\xi)}\right)^{-\epsilon} \hat{P}^{ss'}_{a_i\to(*)}(\xi, \hat{k}_\perp; \epsilon) \Theta(r_{\rm cut} - r^{\mathcal{F}_i^c}) \,,\end{aligned} \tag{2.34}$$

where we have introduced $Q = \sqrt{q^2}$ and $\tilde{x}_i = \tilde{s}_i/Q^2$. Notice that, at leading power, we can safely neglect the invariant mass $\tilde{s}_i$ in the phase space element $d\Pi_n^d$, which, thus, reduces to the Born-like phase space element for n final-state massless partons and a colourless system F. With abuse of notation, we replace $\tilde{p}_i$ with p_i everywhere so that the collection $(p_F, \{p_j\}_{j=2}^{n+2})$ stands for a set of Born momenta. Finally, the full final-state collinear contribution $\mathcal{F}^c$ is obtained by summing over all collinear limits

$$\mathcal{F}^c = \sum_{\mathcal{A}} \sum_{i=3}^{n+2} \int_0^1 dx_1 f_{a_1}(x_1,\mu_F) \int_0^1 dx_2 f_{a_2}(x_2,\mu_F) \int \frac{d\Pi_n^d(q; p_F, \{p_j\})}{2Q^2} \mathcal{I}_{a_1 a_2; a_i} \,, \tag{2.35}$$

where we introduced

$$\mathcal{I}_{a_1 a_2; a_i} = \mathcal{T}^{ss'}_{a_1 a_2;\dots a_i\dots} \mathcal{J}^{ss'}_{a_i}(r_{\rm cut}) \,. \tag{2.36}$$

In the previous formula

$$\begin{aligned}\mathcal{J}^{ss'}_{a_i}(r_{\rm cut}) = &\left(\frac{\mu_R^2}{Q^2}\right)^\epsilon \frac{e^{\gamma_E \epsilon}}{\Gamma(1-\epsilon)} \frac{\alpha_{\rm S}(\mu_R)}{\pi} \sum_{(*)} \int \frac{d\Omega_{d-2}}{\Omega_{d-2}} \int_0^1 d\xi\, \xi^{-\epsilon}(1-\xi)^{-\epsilon} \\ &\times \int_0^{4(p_i^0)^2/Q^2\xi(1-\xi)} dx_i x_i^{-1-\epsilon} \left(1 - \frac{Q^2}{4(p_i^0)^2} \frac{x_i}{\xi(1-\xi)}\right)^{-\epsilon} \hat{P}^{ss'}_{a_i\to(*)}(\xi, \hat{k}_\perp; \epsilon) \Theta(r_{\rm cut} - r^{\mathcal{F}_i^c})\end{aligned} \tag{2.37}$$

is the cumulant NLO jet function. In appendix D we outline a different approach, based on the method of regions, to define jet functions.

2.4 Soft limit

The last singular region we need to consider is the soft one. We observe that our construction leads unavoidably to overlaps among the different soft and collinear approximations. We take care of removing any double counting in the soft contribution $\mathcal{S}^{wa}$ by defining a "subtracted" soft current $\mathbf{J}^2_{\rm sub}$ from which the soft limits of all initial- and final-state collinear approximations have been subtracted. A similar strategy has been used in refs. [78–80]. More precisely, we write the ensuing contribution below the cut as

$$\mathcal{S}^{wa} \equiv \frac{\alpha_{\rm S}(\mu_R)}{\pi} \sum_{\mathcal{A}} \int_0^1 dx_1 f_{a_1}(x_1,\mu_F) \int_0^1 dx_2 f_{a_2}(x_2,\mu_F) \int \frac{d\Pi_n^d(q; p_F, \{p_j\})}{2Q^2} \langle \mathcal{M}^{(0)}_{\mathcal{A}} | \, \mathbf{S} \, | \mathcal{M}^{(0)}_{\mathcal{A}} \rangle \tag{2.38}$$

JHEP12(2023)193

in terms of the NLO soft function

$$\mathbf{S} = 2\mu_R^{2\epsilon} \frac{e^{\gamma_E \epsilon}}{\Gamma(1-\epsilon)} \int \frac{d^d k}{\Omega_{d-2}} \delta_+(k^2) \mathbf{J}^2_{\text{sub}} \,. \tag{2.39}$$

In the above equation, the soft subtracted current is defined as

$$\begin{aligned} \mathbf{J}^2_{\text{sub}} = &\left(-\mathbf{T}_1 \cdot \mathbf{T}_2 \omega_{12} - \sum_i (\mathbf{T}_1 \cdot \mathbf{T}_i \omega_{1i} + (1 \leftrightarrow 2)) - \sum_{i>j} \mathbf{T}_i \cdot \mathbf{T}_j \omega_{ij} \right) \Theta(r_{\text{cut}} - r_S) \\ &- \left(\mathbf{T}_1^2 \omega_2^1 \Theta(r_{\text{cut}} - r_{C_1,S}) + (1 \leftrightarrow 2) \right) - \sum_i \mathbf{T}_i^2 \omega_{C_i,S} \Theta(r_{\text{cut}} - r_{C_i,S}) \,, \end{aligned} \tag{2.40}$$

in terms of the eikonal kernels $\omega_{\alpha\beta}$ and ω_β^α given by

$$\omega_{\alpha\beta} \equiv \frac{p_\alpha \cdot p_\beta}{(k \cdot p_\alpha)(k \cdot p_\beta)} = \omega_\beta^\alpha + \omega_\alpha^\beta \,, \qquad \omega_\beta^\alpha \equiv \frac{p_\alpha \cdot p_\beta}{(k \cdot p_\alpha)(k \cdot (p_\alpha + p_\beta))} \qquad \forall \alpha, \beta = 1, \ldots, n+2 \tag{2.41}$$

and of the soft limit of the final-state splitting kernels $\omega_{C_i,S}$ given by

$$\omega_{C_i,S} \equiv \frac{p_i \cdot (p_1 + p_2)}{(k \cdot p_i)(k \cdot (p_1 + p_2))} \qquad \forall i = 3, \ldots, n+2 \,. \tag{2.42}$$

In eq. (2.40), r_S is the soft limit of the slicing variable, whereas $r_{C_\alpha,S}$ refers to the soft limit of the respective α-collinear approximation of r.

We observe that the first line in eq. (2.40) corresponds to the standard eikonal contribution $\mathbf{J}^2 = -\sum \mathbf{T}_\alpha \cdot \mathbf{T}_\beta \omega_{\alpha\beta}$, while the second line corresponds to the collinear singular contributions that are explicitly subtracted in order to obtain the purely soft wide-angle remainder. The resulting soft function is a well-defined quantity in d dimensions. This is to be contrasted with soft functions defined in SCET, which may require the introduction of suitable rapidity regulators, see e.g. the calculation of one-loop soft functions for N-jet processes at hadron colliders discussed in ref. [81]. Note that the kernels ω_β^α and $\omega_{C_i,S}$, corresponding to the soft limit of the Altarelli-Parisi splitting functions, take the explicit form given in eq. (2.41) and (2.42) as a consequence of our use of the energy fractions z and ξ in the initial-state and final-state collinear regions, respectively.

2.5 Virtual contribution

The virtual diagrams always contribute to the region below the slicing cut, r_{cut}, since, by definition, a proper slicing variable vanishes on a Born-like kinematic configuration. The $\overline{\text{MS}}$ renormalised on-shell scattering amplitude $|\mathcal{M}_{\mathcal{A}}(\mu_R^2, \{p_\alpha\})\rangle$ can be perturbatively expanded as[5]

$$|\mathcal{M}_{\mathcal{A}}(\mu_R^2, \{p_\alpha\})\rangle = |\mathcal{M}_{\mathcal{A}}^{(0)}(\{p_\alpha\})\rangle + \frac{\alpha_{\text{S}}(\mu_R)}{\pi} |\mathcal{M}_{\mathcal{A}}^{(1)}(\mu_R^2, \{p_\alpha\})\rangle + \mathcal{O}(\alpha_{\text{S}}^2) \,. \tag{2.43}$$

It is related to the IR-finite amplitude $|\mathcal{M}_{\mathcal{A}}^{\text{fin}}(\mu_R^2, \{p_\alpha\})\rangle$ via

$$|\mathcal{M}_{\mathcal{A}}^{\text{fin}}(\mu_R^2, \{p_\alpha\})\rangle = [1 - \mathbf{I}(\epsilon, \mu_R^2, \{p_\alpha\})] \, |\mathcal{M}_{\mathcal{A}}(\mu_R^2, \{p_\alpha\})\rangle \,, \tag{2.44}$$

[5] The overall dependence on $\alpha_{\text{S}}(\mu_R)$ entering at Born level is understood.

JHEP12(2023)193

where $\mathbf{I}(\epsilon, \mu_R^2, \{p_\alpha\})$ is the IR subtraction operator that admits the perturbative expansion

$$\mathbf{I}(\epsilon, \mu_R^2, \{p_\alpha\}) = \frac{\alpha_S(\mu_R)}{\pi}\mathbf{I}^{(1)}(\epsilon, \mu_R^2, \{p_\alpha\}) + \mathcal{O}(\alpha_S^2)\,. \tag{2.45}$$

In particular, we are interested in the one-loop finite remainder

$$|\mathcal{M}_{\mathcal{A}}^{(1),\text{fin}}(\mu_R^2, \{p_\alpha\})\rangle = |\mathcal{M}_{\mathcal{A}}^{(1)}(\mu_R^2, \{p_\alpha\})\rangle - \mathbf{I}^{(1)}(\epsilon, \mu_R^2, \{p_\alpha\})\,|\mathcal{M}_{\mathcal{A}}^{(0)}(\{p_\alpha\})\rangle\ , \tag{2.46}$$

where $\mathbf{I}^{(1)}$ embodies the IR singular structure of the one-loop amplitude [12, 61, 82]. The explicit expression of $\mathbf{I}^{(1)}(\epsilon, \mu_R^2, \{p_\alpha\})$ is

$$\begin{aligned}
&\mathbf{I}^{(1)}(\epsilon, \mu_R^2, \{p_\alpha\}) = \\
&\left(\frac{\mu_R^2}{Q^2}\right)^{\epsilon} \frac{e^{\gamma_E \epsilon}}{\Gamma(1-\epsilon)}\frac{1}{4}\Bigg\{\sum_{\alpha\in\mathcal{A}}\left(-\frac{C_\alpha}{\epsilon^2} - \frac{2}{\epsilon}\gamma_\alpha\right) - \frac{2}{\epsilon}i\pi\mathbf{T}_1\cdot\mathbf{T}_2 \\
&\quad + \frac{2}{\epsilon}\sum_i \mathbf{T}_i\cdot\left[\mathbf{T}_1\log\left(\frac{Q^2}{2p_1\cdot p_i}\right) + \mathbf{T}_2\log\left(\frac{Q^2}{2p_2\cdot p_i}\right)\right] + \frac{1}{\epsilon}\sum_{i\neq j}\mathbf{T}_i\cdot\mathbf{T}_j\left[\log\left(\frac{Q^2}{2p_i\cdot p_j}\right) - i\pi\right]\Bigg\},
\end{aligned} \tag{2.47}$$

where the coefficients γ_q and γ_g are defined in eq. (2.26). It is useful to introduce the hard function

$$H(\alpha_S(Q)) = 1 + \frac{\alpha_S(Q)}{\pi}H^{(1)} + \mathcal{O}(\alpha_S^2)\,, \tag{2.48}$$

where the $\mathcal{O}(\alpha_S)$ contribution is

$$H^{(1)} \equiv \frac{\langle\mathcal{M}_{\mathcal{A}}^{(0)}(\{p_\alpha\})\,|\mathcal{M}_{\mathcal{A}}^{(1),\text{fin}}(\mu_R^2 = Q^2, \{p_\alpha\})\rangle + \text{c.c.}}{|\mathcal{M}_{\mathcal{A}}^{(0)}(\{p_\alpha\})|^2}\,, \tag{2.49}$$

which is evaluated in $d = 4$ dimensions. The one-loop contribution to the NLO cross section is

$$\begin{aligned}
\mathcal{V} \equiv{}& \frac{\alpha_S(\mu_R)}{\pi}\sum_{\mathcal{A}}\int_0^1 dx_1 f_{a_1}(x_1, \mu_F)\int_0^1 dx_2 f_{a_2}(x_2, \mu_F) \\
&\times\int\frac{d\Pi_n^d(q; p_F, \{p_j\})}{2Q^2}\left(\langle\mathcal{M}_{\mathcal{A}}^{(0)}(\{p_\alpha\})\,|\mathcal{M}_{\mathcal{A}}^{(1)}(\mu_R^2, \{p_\alpha\})\rangle + \text{c.c.}\right)\,,
\end{aligned} \tag{2.50}$$

where $\mathcal{A} = \{a_1, a_2, \{a_i\}\}$ and

$$\begin{aligned}
\langle\mathcal{M}_{\mathcal{A}}^{(0)}(\{p_\alpha\})\,|\mathcal{M}_{\mathcal{A}}^{(1)}(\mu_R^2, \{p_\alpha\})\rangle + \text{c.c.} = \Big(&\langle\mathcal{M}_{\mathcal{A}}^{(0)}(\{p_\alpha\})|\,\mathbf{I}^{(1)}(\epsilon, \mu_R^2, \{p_\alpha\})\,|\mathcal{M}_{\mathcal{A}}^{(0)}(\{p_\alpha\})\rangle \\
&+ \langle\mathcal{M}_{\mathcal{A}}^{(0)}(\{p_\alpha\})\,|\mathcal{M}_{\mathcal{A}}^{(1),\text{fin}}(\mu_R^2, \{p_\alpha\})\rangle\Big) + \text{c.c.}\,.
\end{aligned} \tag{2.51}$$

The manifest ϵ-poles in the one-loop contribution cancel against those generated by the integration of the real contribution over the radiation phase space, which are explicitly contained in the beam, jet and soft functions. The remaining singularities are of pure

JHEP12(2023)193

initial-state collinear origin and are cancelled by the $\overline{\text{MS}}$ counterterm associated with the renormalisation of the PDFs, which reads

$$\mathcal{C}_{\overline{\text{MS}}} \equiv \sum_{\mathcal{A}} \sum_{\{b_1,b_2\}} \int_0^1 dx_1 \int_0^1 dx_2 \int \frac{d\Pi_n^d(q;p_F,\{p_j\})}{2Q^2} \left(\frac{\mu_R^2}{\mu_F^2}\right)^{\epsilon} \frac{e^{\gamma_E \epsilon}}{\Gamma(1-\epsilon)} \frac{\alpha_S(\mu_R)}{\pi} |\mathcal{M}_{\mathcal{A}}^{(0)}|^2 \frac{1}{\epsilon}$$
$$\times \int_{x_1}^1 \frac{dz_1}{z_1} \int_{x_2}^1 \frac{dz_2}{z_2} \left(P_{a_1 b_1}(z_1;\epsilon=0)\delta_{a_2 b_2}\delta(1-z_2) + (1 \leftrightarrow 2) \right) f_{b_1}\left(\frac{x_1}{z_1},\mu_F\right) f_{b_2}\left(\frac{x_2}{z_2},\mu_F\right). \tag{2.52}$$

3 Applications

In this section we apply the general formalism discussed in section 2 to two candidate variables for jet hadroproduction processes, the one-jet resolution variable ΔE_t and the n-jet resolution variable k_T^{ness}. We start by presenting explicit analytic results for both observables in section 3.1 and 3.2, respectively. Finally, in section 3.3 we present NLO numerical results for specific processes obtained using both slicing variables.

3.1 ΔE_t slicing

We start by considering a variable relevant for the class of processes in which a colourless system F is produced in association with a hard jet of momentum p_J. For these processes a possible resolution variable can be defined as follows. Considering an event in which F is accompanied by m QCD partons with momenta $p_3, \ldots, p_{m+2}$, we define

$$\Delta E_t = \sum_{i=3}^{m+2} |\vec{p}_{i,t}| - |\vec{p}_{F,t}|\,. \tag{3.1}$$

At LO we have $m = 1$, implying that $\Delta E_t = 0$ for the Born and one-loop contributions, while for real-emission diagrams we have $m = 2$. Momentum conservation and the triangle inequality imply that ΔE_t is non-negative and it vanishes only when all $\vec{p}_{i,t}$ are either zero or antiparallel to $\vec{p}_{F,t}$. As a consequence, at NLO, real-emission diagrams lead to $\Delta E_t = 0$ in the soft and/or collinear limits.

Thus, we can define the dimensionless slicing variable

$$r = \frac{\Delta E_t}{Q} \tag{3.2}$$

where $Q^2 = (p_F + p_J)^2$ is the squared invariant mass of the Born-like system.[6] The variable ΔE_t defined above is not expected to feature non-global logarithmic contributions [65] and can be evaluated without relying on a jet algorithm. Therefore, it can be potentially useful to deal with the class of processes in which a colourless system F is produced in association with a hard jet. We will show in the following that this variable presents a richer structure compared to the one associated with q_T or 1-jettiness. In view of these interesting features, the necessary ingredients to construct a slicing method turn out to be more difficult to evaluate.

[6] p_J can be determined with an arbitrary exclusive (always giving us exactly one jet) IR-safe jet-clustering algorithm. The choice of the algorithm will only affect the power corrections in r_{cut}.

JHEP12(2023)193

In particular, ΔE_t features a non-trivial azimuthal dependence which is responsible for the presence of non-vanishing spin correlations, already at NLO, and of additional initial-state collinear contributions with respect to those appearing in q_T-subtraction.

3.1.1 Initial-state collinear limit

In the limit in which the radiated parton of momentum k is collinear to the beams ($k_t \to 0$), we can write the transverse momentum of the final-state hard parton p_3 as

$$|\vec{p}_{3,t}| = |\vec{p}_{F,t} + \vec{k}_t| = \sqrt{|\vec{p}_{F,t}|^2 + |\vec{k}_t|^2 + 2|\vec{p}_{F,t}||\vec{k}_t|\cos\phi} \approx |\vec{p}_{F,t}|\left(1 + \frac{|\vec{k}_t|}{|\vec{p}_{F,t}|}\cos\phi\right) \tag{3.3}$$

by neglecting quadratic terms in k_t. From this approximation, the normalised slicing parameter is

$$r^{\mathcal{I}^c} = r^{\mathcal{I}^c_1} = r^{\mathcal{I}^c_2} \equiv \frac{\Delta E_t^{\mathcal{I}^c}}{Q} \approx \frac{|\vec{p}_{F,t}|}{Q}\left(1 + \frac{|\vec{k}_t|}{|\vec{p}_{F,t}|}\cos\phi\right) + |\vec{k}_t| - |\vec{p}_{F,t}| = \frac{k_t}{Q}(1+\cos\phi)\,. \tag{3.4}$$

For the sake of comparison, we introduce a simple power counting in terms of the energy of the emitted parton E and of the angle θ it forms with the relevant collinear direction. In this region, we notice that the variable scales as $\Delta E_t^{\mathcal{I}^c} \sim E\theta$, which is the same scaling as q_T.

By exploiting the parametrisation outlined in section 2.2, the initial-state collinear contribution in eq. (2.20) can be evaluated. The function $\mathcal{I}^{b_1 b_2}_{a_1 a_2}(z_1, z_2)$ in eq. (2.21) reduces to

$$\begin{aligned}
\mathcal{I}^{b_1 b_2}_{a_1 a_2}(z_1, z_2) = &\left(\frac{\mu_R^2}{Q^2}\right)^{\epsilon} \frac{e^{\gamma_E \epsilon}}{\Gamma(1-\epsilon)} \frac{\alpha_S(\mu_R)}{\pi} |\mathcal{M}^{(0)}_{\mathcal{A}}|^2 \\
&\times \Bigg\{ \Bigg[\left(\frac{1}{2\epsilon^2} - \log^2(2r_{\text{cut}}) - \frac{\pi^2}{3}\right) C_{a_1}\delta_{a_1 b_1}\delta_{a_2 b_2}\delta(1-z_1)\delta(1-z_2) \\
&+ \left(-\frac{1}{\epsilon} + 2\log(2r_{\text{cut}})\right)\left(-\gamma_{a_1}\delta_{a_1 b_1}\delta(1-z_1) + P_{a_1 b_1}(z_1;\epsilon=0)\right)\delta_{a_2 b_2}\delta(1-z_2) \\
&+ C_{a_1 b_1}(z_1)\delta_{a_2 b_2}\delta(1-z_2) + (1 \leftrightarrow 2)\Bigg] \\
&+ \left[G_{a_1 b_1}(z_1)\delta_{a_1 g}\delta_{a_2 b_2}\delta(1-z_2)\left(\frac{|\mathcal{M}^{(0),\epsilon_1}_{\mathcal{A}}|^2}{|\mathcal{M}^{(0)}_{\mathcal{A}}|^2} - \frac{|\mathcal{M}^{(0),\epsilon_2}_{\mathcal{A}}|^2}{|\mathcal{M}^{(0)}_{\mathcal{A}}|^2}\right) + (1 \leftrightarrow 2)\right]\Bigg\}\,,
\end{aligned} \tag{3.5}$$

where $C_{ab}(z)$, $G_{ab}(z)$ and the regularised Altarelli-Parisi splitting kernels $P_{ab}(z)$ are defined in appendix B. The spin-polarised matrix element, $|\mathcal{M}^{(0),\epsilon_i}_{\mathcal{A}}|^2$, is given by

$$|\mathcal{M}^{(0),\epsilon_i}_{\mathcal{A}}|^2 = \mathcal{T}^{\mu\nu}_{\mathcal{A}}\epsilon_{i,\mu}\epsilon_{i,\nu}\,, \tag{3.6}$$

where the gluon a_1 is polarised along ϵ_i^μ, with $i \in \{1,2\}$. Here, ϵ_1^μ is the transverse polarisation of the gluon along the transverse momentum of the colourless system with respect to the beam (i.e. $p_{F,t}$) and ϵ_2^μ is the transverse polarisation orthogonal to ϵ_1^μ. More details on the spin-polarised matrix elements $|\mathcal{M}^{(0),\epsilon_i}_{\mathcal{A}}|^2$ are provided in appendix A.

JHEP12(2023)193

The corresponding cumulant beam function in eq. (2.22) reads

$$\begin{aligned}\mathcal{B}_{ab}^{ss'}(z, r_{\rm cut}) = \left(\frac{\mu_R^2}{Q^2}\right)^{\epsilon} \frac{e^{\gamma_E \epsilon}}{\Gamma(1-\epsilon)} \frac{\alpha_{\rm S}(\mu_R)}{\pi} \Bigg\{ d_a^{ss'} \Bigg[\left(\frac{1}{2\epsilon^2} - \log^2(2r_{\rm cut}) - \frac{\pi^2}{3}\right) C_a \delta_{ab} \delta(1-z) \\ + \left(-\frac{1}{\epsilon} + 2\log(2r_{\rm cut})\right) \Big(-\gamma_a \delta_{ab} \delta(1-z) + P_{ab}(z; \epsilon=0)\Big) + C_{ab}(z) \Bigg] \\ + G_{ab}(z) \delta_{ag} \mathcal{A}^{ss'} \Bigg\}, \end{aligned} \tag{3.7}$$

where $d_a^{ss'}$ is given in eq. (2.24) and the asymmetry tensor $\mathcal{A}^{ss'}$ is defined in appendix A. We see that ΔE_t features a non-trivial azimuthal dependence which is responsible for the presence of non-vanishing spin-correlations, driven by $\mathcal{A}^{ss'}$ (see eq. (A.12)), already at this perturbative order. Such contributions are new with respect to those appearing in q_T-subtraction. This feature is analogous to what happens for the variable considered in ref. [83].

3.1.2 Final-state collinear limit

In the following, frame-dependent quantities are specified in the partonic CM frame. By using the parametrisation outlined in section 2.3, we find that the slicing variable can be approximated as

$$r^{\mathcal{F}^c} = \frac{\Delta E_t^{\mathcal{F}^c}}{Q} = \frac{Q}{2p_{J,t}} x_3 \sin^2\varphi \tag{3.8}$$

in the final-state collinear limit, where the angle between p_3 and k goes to 0. Here, $\cos\varphi = \frac{\vec{p}_{1,\perp}\cdot\vec{k}_\perp}{p_{1,\perp}k_\perp}$, where $\vec{v}_\perp$ is obtained by projecting the spatial part of a four-vector v onto the transverse plane of $\vec{p}_J$, and $p_{J,t}$ is the transverse momentum of the jet p_J with respect to the beam direction. We notice that in this region the variable scales as $\Delta E_t^{\mathcal{F}^c} \sim E\theta^2$, which is the same scaling as N-jettiness in any collinear limit. Thus, the variable scales differently in the initial- and final-state collinear regions. Finally, the final-state collinear contribution in eq. (2.35) can be evaluated. The function $\mathcal{I}_{a_1 a_2; a}$ in eq. (2.36) is found to be

$$\begin{aligned}\mathcal{I}_{a_1 a_2; a} = \left(\frac{\mu_R^2}{Q^2}\right)^{\epsilon} \frac{e^{\gamma_E \epsilon}}{\Gamma(1-\epsilon)} \frac{\alpha_{\rm S}(\mu_R)}{\pi} |\mathcal{M}_{\mathcal{A}}^{(0)}|^2 \Bigg\{ \frac{1}{6}\left(\frac{C_A}{2} - T_R n_f\right) \left(\frac{|\mathcal{M}_{\mathcal{A}}^{(0),\varepsilon_1}|^2}{|\mathcal{M}_{\mathcal{A}}^{(0)}|^2} - \frac{|\mathcal{M}_{\mathcal{A}}^{(0),\varepsilon_2}|^2}{|\mathcal{M}_{\mathcal{A}}^{(0)}|^2}\right) \delta_{ag} \\ - \gamma_a \left(-\frac{1}{\epsilon} + \log(8r_{\rm cut}) + \frac{1}{2}\log\frac{p_{J,t}^2}{Q^2}\right) + \chi_a \\ + C_a \Bigg[\frac{1}{2\epsilon^2} - \frac{1}{2}\log^2(8r_{\rm cut}) - \frac{1}{2}\log\frac{4E_J^2}{Q^2}\left(\frac{1}{\epsilon} - 2\log(8r_{\rm cut})\right) - \frac{1}{2}\log\frac{p_{J,t}^2}{Q^2}\log(8r_{\rm cut}) \\ + \frac{1}{8}\log^2\frac{p_{J,t}^2}{Q^2} - \frac{1}{4}\left(\log\frac{p_{J,t}^2}{Q^2} - \log\frac{4E_J^2}{Q^2}\right)^2 \Bigg] \Bigg\}, \end{aligned} \tag{3.9}$$

where $E_J = \frac{p_J\cdot(p_1+p_2)}{Q}$ is the jet energy and we defined the constants

$$\chi_q = C_F\left(\frac{7}{4} - \frac{5}{12}\pi^2\right), \qquad \chi_g = \left(\frac{67}{36} - \frac{5}{12}\pi^2\right) C_A - \frac{5}{9} T_R n_f\,. \tag{3.10}$$

JHEP12(2023)193

$|\mathcal{M}_{\mathcal{A}}^{(0),\varepsilon_i}|^2$ is the spin-polarised matrix element

$$|\mathcal{M}_{\mathcal{A}}^{(0),\varepsilon_i}|^2 = \mathcal{T}_{\mathcal{A}}^{\mu\nu}\varepsilon_{i,\mu}\varepsilon_{i,\nu}\,, \tag{3.11}$$

where the gluon a is polarised along ε_i^μ with $i \in \{1,2\}$. Here, ε_1^μ is the transverse polarisation of the gluon along the transverse momentum of the beam with respect to the jet (i.e. $p_{1,\perp}$) and ε_2^μ is the transverse polarisation orthogonal to ε_1^μ. More details on the spin polarised matrix elements $|\mathcal{M}_{\mathcal{A}}^{(0),\varepsilon_i}|^2$ are provided in appendix A.

The corresponding cumulant jet function in eq. (2.37) reads

$$\begin{aligned}\mathcal{J}_a^{ss'}(r_{\text{cut}}) = \left(\frac{\mu_R^2}{Q^2}\right)^{\epsilon}\frac{e^{\gamma_E\epsilon}}{\Gamma(1-\epsilon)}\frac{\alpha_{\text{S}}(\mu_R)}{\pi}\Bigg\{&\frac{1}{6}\left(\frac{C_A}{2}-T_R n_f\right)\mathcal{A}^{ss'}\delta_{ag}\\
&+ d_a^{ss'}\Bigg[-\gamma_a\left(-\frac{1}{\epsilon}+\log(8r_{\text{cut}})+\frac{1}{2}\log\frac{p_{J,t}^2}{Q^2}\right)+\chi_a\\
&+C_a\left(\frac{1}{2\epsilon^2}-\frac{1}{2}\log^2(8r_{\text{cut}})-\frac{1}{2}\log\frac{4E_J^2}{Q^2}\left(\frac{1}{\epsilon}-2\log(8r_{\text{cut}})\right)-\frac{1}{2}\log\frac{p_{J,t}^2}{Q^2}\log(8r_{\text{cut}})\right.\\
&\left.+\frac{1}{8}\log^2\frac{p_{J,t}^2}{Q^2}-\frac{1}{4}\left(\log\frac{p_{J,t}^2}{Q^2}-\log\frac{4E_J^2}{Q^2}\right)^2\right)\Bigg]\Bigg\}\,,\end{aligned} \tag{3.12}$$

where $d_a^{ss'}$ is given in eq. (2.24) and the asymmetry tensor $\mathcal{A}^{ss'}$ is defined in appendix A. We see that the non-trivial azimuthal dependence of ΔE_t is responsible for non-vanishing spin-correlations also in this contribution. As for the case of the initial-state collinear limit, this feature is analogous to what happens for the variable considered in ref. [83].

3.1.3 Soft limit

In the soft limit, ΔE_t assumes the same expression (and, therefore, the same scaling in the soft-collinear limit) as the one derived in the initial-state collinear region, i.e. $r_S = r_{C_1,S} = r_{C_2,S} = \frac{k_t}{Q}(1+\cos\phi)$. We also need to specify the soft limit of the approximation we used in the final-state collinear region, which is given by $r_{C_3,S} = \frac{k\cdot p_3}{p_{J,t}}\frac{\sin^2\varphi}{Q}$.

By exploiting the results of section 2.4, the soft-subtracted contribution below the slicing cut, r_{cut}, can be written as

$$\begin{aligned}\mathcal{S}^{wa} = -\frac{\alpha_{\text{S}}(\mu_R)}{\pi}\sum_{\mathcal{A}}\int_0^1 dx_1 f_{a_1}(x_1,\mu_F)\int_0^1 dx_2 f_{a_2}(x_2,\mu_F)\times\\
\times\int\frac{d\Pi_1^d(p_1+p_2;p_F,p_J)}{2Q^2}\,\langle\mathcal{M}_{\mathcal{A}}^{(0)}|\left[\mathbf{T}_1\cdot\mathbf{T}_3\,\mathcal{S}_{13}+\mathbf{T}_2\cdot\mathbf{T}_3\,\mathcal{S}_{23}\right]|\mathcal{M}_{\mathcal{A}}^{(0)}\rangle\end{aligned} \tag{3.13}$$

where $\mathcal{A} = \{a_1, a_2, a\}$ labels the different Born channels $a_1 + a_2 \to a + F$. The soft integral $\mathcal{S}_{13}$ is defined as

$$\begin{aligned}\mathcal{S}_{13} = 2\mu_R^{2\epsilon}\frac{e^{\gamma_E\epsilon}}{\Gamma(1-\epsilon)}\int\frac{d^dk}{\Omega_{d-2}}\,\delta_+(k^2)\Bigg\{&\left(\frac{p_1\cdot p_J}{k\cdot p_1 k\cdot p_J}-\frac{p_1\cdot p_2}{k\cdot p_1 k\cdot(p_1+p_2)}\right)\Theta\left(r_{\text{cut}}-r_S\right)\\
&-\frac{(p_1+p_2)\cdot p_J}{k\cdot(p_1+p_2)k\cdot p_J}\Theta\left(r_{\text{cut}}-r_{C_3,S}\right)\Bigg\}\,,\end{aligned} \tag{3.14}$$

and $\mathcal{S}_{23} = \mathcal{S}_{13}(p_1 \leftrightarrow p_2)$.

JHEP12(2023)193

After performing the integration over the radiation phase space, we obtain

$$\mathcal{S}_{13} = \left(\frac{\mu_R^2}{Q^2}\right)^{\epsilon} \frac{e^{\gamma_E \epsilon}}{\Gamma(1-\epsilon)} \left\{ \left(\frac{1}{\epsilon} - 2\log(8 r_{\text{cut}})\right) \left(\eta_J - \frac{1}{2}\log\frac{p_{J,t}^2}{Q^2} + \frac{1}{2}\log\frac{4E_J^2}{Q^2}\right) + \frac{\pi^2}{12} + 4\log 2\,(\eta_J + \log 2) + \frac{1}{4}\left(\log\frac{p_{J,t}^2}{Q^2} - \log\frac{4E_J^2}{Q^2}\right)^2 \right\}, \quad (3.15)$$

where the jet rapidity is

$$\eta_J = \frac{1}{2}\log\left(\frac{p_2 \cdot p_J}{p_1 \cdot p_J}\right). \quad (3.16)$$

3.1.4 Subtraction coefficients for ΔE_t slicing

By adding all contributions we computed in the previous sections, we manage to cancel the IR singular poles and we can now extract the expression for the $\mathbf{\Sigma}^{1k}$ functions introduced in section 2.1:

$$\mathbf{\Sigma}^{12}_{\mathcal{A} b_1 b_2}(z_1, z_2) = \delta_{a_1 b_1}\delta_{a_2 b_2}\delta(1-z_1)\delta(1-z_2)\left\{-C_{a_1} - C_{a_2} - \frac{C_a}{2}\right\}\mathbf{1} \quad (3.17)$$

$$\begin{aligned}\mathbf{\Sigma}^{11}_{\mathcal{A} b_1 b_2}(z_1, z_2) = {} & 2\Big(P_{a_1 b_1}(z_1; \epsilon = 0)\delta_{a_2 b_2}\delta(1-z_2) + (1 \leftrightarrow 2)\Big)\mathbf{1} \\ & + \delta_{a_1 b_1}\delta_{a_2 b_2}\delta(1-z_1)\delta(1-z_2)\left\{-(2\gamma_{a_1} + 2\gamma_{a_2} + \gamma_a) + \frac{C_a}{2}\log\frac{p_{J,t}^2}{Q^2}\right. \\ & \left. - 2(C_A - C_F)(\delta_{a_1 g} - \delta_{a_2 g})\eta_J - (2C_{a_1} + 2C_{a_2} + 3C_a)\log 2\right\}\mathbf{1}\end{aligned} \quad (3.18)$$

$$\begin{aligned}\mathbf{\Sigma}^{10}_{\mathcal{A} b_1 b_2}(z_1, z_2) = {} & \left[\log\left(\frac{Q^2}{\mu_F^2}\right) + 2\log 2\right]\Big(P_{a_1 b_1}(z_1; \epsilon = 0)\delta_{a_2 b_2}\delta(1-z_2) + (1 \leftrightarrow 2)\Big)\mathbf{1} \\ & + \Big(C_{a_1 b_1}(z_1)\delta_{a_2 b_2}\delta(1-z_2) + (1 \leftrightarrow 2)\Big)\mathbf{1} \\ & + \left(G_{a_1 b_1}(z_1)\delta_{a_1 g}\delta_{a_2 b_2}\delta(1-z_2)\left(\frac{|\mathcal{M}^{(0),\epsilon_1}_{\mathcal{A}}|^2}{|\mathcal{M}^{(0)}_{\mathcal{A}}|^2} - \frac{|\mathcal{M}^{(0),\epsilon_2}_{\mathcal{A}}|^2}{|\mathcal{M}^{(0)}_{\mathcal{A}}|^2}\right) + (1 \leftrightarrow 2)\right)\mathbf{1} \\ & + \delta_{a_1 b_1}\delta_{a_2 b_2}\delta(1-z_1)\delta(1-z_2)\left\{H^{(1)} - p_B\beta_0\log\left(\frac{Q^2}{\mu_R^2}\right)\right. \\ & - \left(C_{a_1} + C_{a_2} + \frac{C_a}{2}\right)\log^2 2 \\ & + \left(-(2\gamma_{a_1} + 2\gamma_{a_2} + 3\gamma_a) + 2(C_F - C_A)(\delta_{a_1 g} - \delta_{a_2 g})\eta_J + \frac{3}{2}C_a\log\frac{p_{J,t}^2}{Q^2}\right)\log 2 \\ & + \frac{C_a}{8}\log^2\frac{p_{J,t}^2}{Q^2} - \frac{\gamma_a}{2}\log\frac{p_{J,t}^2}{Q^2} + \chi_a - \left(C_{a_1} + C_{a_2} - \frac{C_a}{4}\right)\frac{\pi^2}{3} \\ & \left. + \frac{1}{6}\left(\frac{C_A}{2} - T_R n_f\right)\delta_{ag}\left(\frac{|\mathcal{M}^{(0),\varepsilon_1}_{\mathcal{A}}|^2}{|\mathcal{M}^{(0)}_{\mathcal{A}}|^2} - \frac{|\mathcal{M}^{(0),\varepsilon_2}_{\mathcal{A}}|^2}{|\mathcal{M}^{(0)}_{\mathcal{A}}|^2}\right)\right\}\mathbf{1}\,,\end{aligned} \quad (3.19)$$

where p_B denotes the power of $\alpha_S(\mu_R)$ that appears in the LO cross section.

JHEP12(2023)193

We note that, for a final-state emitter l, the contribution to the double logarithm in r_{cut} is proportional to the Casimir (C_l) associated with the respective leg and it corresponds to half of the contribution from an initial-state leg. This can be traced back to the different scaling behaviour of the slicing variable in the soft collinear limits. If the variable scales as $E^{a_l}\theta^{b_l}$ in the limit in which the single emission is soft and collinear to leg l, this singular limit contributes to the coefficient of the double logarithm with a factor $-\frac{C_l}{a_l b_l}$. In the specific case of ΔE_t, it turns out that $a_l = b_l = 1$ for initial-state radiation and $a_l = 1, b_l = 2$ for final-state radiation.

3.2 k_T^{ness} slicing

We now consider a more general class of processes in which an arbitrary number n of hard jets is produced, possibly in association with a colourless system F. Prominent examples among such processes are di-jet and tri-jet production, or the production of a colourless system in association with one or more hard jets. The k_T^{ness} variable, introduced in ref. [71], takes its name from the k_T-clustering algorithm [84, 85] and it represents an effective transverse momentum, describing the limit in which the additional jet is unresolved. If the unresolved radiation is close to the colliding beams or the event has no jets at Born level, k_T^{ness} reduces to the transverse momentum (q_T) of the hard system. On the other hand, if the unresolved radiation is emitted close to one of the final-state jets, k_T^{ness} describes the relative transverse momentum of the radiation with respect to the jet direction.

As already mentioned, the definition of k_T^{ness} is based on the exclusive k_T-clustering algorithm, which is applied until $n+1$ final-state jets remain. If we are performing an N^{k}LO computation, the role of k_T^{ness} is to discriminate between the fully unresolved region ($k_T^{\text{ness}} = 0$) and the region where at least one additional parton is resolved ($k_T^{\text{ness}} > 0$). In the latter region, the IR-singularity structure can be at most of N^{k-1}LO-type. If we limit ourselves to NLO, the full clustering algorithm is not necessary and the definition of k_T^{ness} directly coincides with the minimum among the usual distances $d_{ij} = \min(p_{i,t}\,, p_{j,t})\Delta R_{ij}/D$ between two particles and the particle-beam distances $d_{iB} = p_{i,t}$. Here D is a parameter of order unity and ΔR_{ij} is the customary ij distance in rapidity and azimuth. For a complete discussion of the recursive definition in the general case, we refer the reader to ref. [71], where more details about the features of k_T^{ness} are also provided. In particular, besides being global, k_T^{ness} turns out to be very stable with respect to hadronisation and multiparton interactions.

We can now define the dimensionless slicing variable

$$r = \frac{k_T^{\text{ness}}}{Q} \tag{3.20}$$

where Q is the invariant mass of the hard system consisting of n jets plus the colourless system. We point out that Q must be an IR-safe quantity, and can for instance be determined by running the same IR-safe exclusive clustering algorithm exploited in the definition of k_T^{ness}, until exactly n jets remain.

3.2.1 Initial-state collinear limit

When the unresolved radiation is collinear to an initial-state parton, k_T^{ness} reduces to the usual transverse momentum of the Born-like system with respect to the beam, and, thus, it

JHEP12(2023)193

scales as $\sim E\theta$. It follows that the normalised slicing parameter can be approximated as

$$r^{\mathcal{I}^c} = r^{\mathcal{I}_1^c} = r^{\mathcal{I}_2^c} \equiv \frac{k_t}{Q}\,. \tag{3.21}$$

By exploiting the parametrisation outlined in section 2.2, the initial-state collinear contribution in eq. (2.20) can be evaluated. The function $\mathcal{I}^{b_1 b_2}_{a_1 a_2}(z_1, z_2)$ in eq. (2.21) reduces to

$$\begin{aligned}\mathcal{I}^{b_1 b_2}_{a_1 a_2}(z_1, z_2) = \left(\frac{\mu_R^2}{Q^2}\right)^{\epsilon} \frac{e^{\gamma_E \epsilon}}{\Gamma(1-\epsilon)} \frac{\alpha_{\rm S}(\mu_R)}{\pi} |\mathcal{M}^{(0)}_{\mathcal{A}}|^2 \\ \times \Bigg\{ \Bigg[\left(\frac{1}{2\epsilon^2} - \log^2(r_{\rm cut})\right) C_{a_1} \delta_{a_1 b_1} \delta_{a_2 b_2} \delta(1-z_1)\delta(1-z_2) \\ + \left(-\frac{1}{\epsilon} + 2\log(r_{\rm cut})\right)\left(-\gamma_{a_1}\delta_{a_1 b_1}\delta(1-z_1) + P_{a_1 b_1}(z_1;\epsilon=0)\right)\delta_{a_2 b_2}\delta(1-z_2) \\ + C_{a_1 b_1}(z_1)\delta_{a_2 b_2}\delta(1-z_2) + (1 \leftrightarrow 2)\Bigg]\Bigg\}\,,\end{aligned} \tag{3.22}$$

where $C_{ab}(z)$ and the regularised Altarelli-Parisi splitting kernels $P_{ab}(z)$ are defined in appendix B. The cumulant beam function in eq. (2.22) reads

$$\begin{aligned}\mathcal{B}^{ss'}_{ab}(z, r_{\rm cut}) = d^{ss'}_a \left(\frac{\mu_R^2}{Q^2}\right)^{\epsilon} \frac{e^{\gamma_E \epsilon}}{\Gamma(1-\epsilon)} \frac{\alpha_{\rm S}(\mu_R)}{\pi} \Bigg\{ \Bigg[\left(\frac{1}{2\epsilon^2} - \log^2(r_{\rm cut})\right) C_a \delta_{ab}\delta(1-z) \\ + \left(-\frac{1}{\epsilon} + 2\log(r_{\rm cut})\right)\left(-\gamma_a \delta_{ab}\delta(1-z) + P_{ab}(z;\epsilon=0)\right) + C_{ab}(z)\Bigg]\Bigg\}\,,\end{aligned} \tag{3.23}$$

where the tensor $d^{ss'}_a$ is defined in eq. (2.24). The result in eq. (3.23) corresponds to the well-known transverse-momentum beam function, which appears in the production of a colourless system [86].

3.2.2 Final-state collinear limit

In the following, frame-dependent quantities are specified in the partonic CM frame. By using the parametrisation outlined in section 2.3, we find that the slicing variable can be approximated as

$$\left(r^{\mathcal{F}_i^c}\right)^2 = \min(\xi^2, (1-\xi)^2) \frac{x_i}{\xi(1-\xi)D^2} \tag{3.24}$$

in the final-state collinear limit, where the angle between p_i and k goes to 0. Here, D is the parameter entering the definition of $k_T^{\rm ness}$. We notice that in this limit the variable scales as $\sim E\theta$, as expected from its definition as an effective transverse momentum with respect to any collinear direction. Thus, $k_T^{\rm ness}$ features a uniform scaling in all initial-state and final-state collinear regions.

Finally, the final-state collinear contribution in eq. (2.35) can be evaluated. The function $\mathcal{I}_{a_1 a_2; a_i}$ in eq. (2.36) is found to be

$$\begin{aligned}\mathcal{I}_{a_1 a_2; a_i} = \left(\frac{\mu_R^2}{Q^2}\right)^{\epsilon} \frac{e^{\gamma_E \epsilon}}{\Gamma(1-\epsilon)} \frac{\alpha_{\rm S}(\mu_R)}{\pi} |\mathcal{M}^{(0)}_{\mathcal{A}}|^2 \Bigg\{ -\gamma_{a_i}\left(-\frac{1}{\epsilon} + 2\log(Dr_{\rm cut}) + 2\log(2)\right) + \kappa_{a_i} \\ + C_{a_i}\left[\frac{1}{2\epsilon^2} - \frac{1}{2\epsilon}\log\frac{4E_{J_i}^2}{Q^2} - \log^2(Dr_{\rm cut}) + \log\frac{4E_{J_i}^2}{Q^2}\log(Dr_{\rm cut})\right]\Bigg\}\,,\end{aligned} \tag{3.25}$$

JHEP12(2023)193

where the coefficients γ_{a_i} are defined in eq. (2.26), $E_{J_i} = \frac{p_i\cdot(p_1+p_2)}{Q}$ is the energy of the i-th jet and we introduced the constants

$$\kappa_q = C_F\left(\frac{7}{4} - \frac{\pi^2}{4}\right), \qquad \kappa_g = \left(\frac{131}{72} - \frac{\pi^2}{4}\right)C_A - \frac{17}{36}T_R n_f\,. \tag{3.26}$$

The corresponding cumulant jet function in eq. (2.37) reads

$$\begin{aligned}\mathcal{J}_{a_i}^{ss'}(r_{\rm cut}) = d_{a_i}^{ss'}\left(\frac{\mu_R^2}{Q^2}\right)^{\epsilon}\frac{e^{\gamma_E\epsilon}}{\Gamma(1-\epsilon)}\frac{\alpha_{\rm S}(\mu_R)}{\pi}\left\{-\gamma_{a_i}\left(-\frac{1}{\epsilon} + 2\log(Dr_{\rm cut}) + 2\log(2)\right) + \kappa_{a_i}\right.\\ \left. + C_{a_i}\left[\frac{1}{2\epsilon^2} - \frac{1}{2\epsilon}\log\frac{4E_{J_i}^2}{Q^2} - \log^2(Dr_{\rm cut}) + \log\frac{4E_{J_i}^2}{Q^2}\log(Dr_{\rm cut})\right]\right\}.\end{aligned} \tag{3.27}$$

3.2.3 Soft limit

In the following, frame-dependent quantities are specified in the partonic CM frame. In the soft limit, $k_T^{\rm ness}$ assumes the expression

$$r_S = \frac{k_{T,S}^{\rm ness}}{Q} = \min(1, \{\Delta R_{i(k)}\}/D)\frac{k_t}{Q}\,, \tag{3.28}$$

where $\Delta R_{i(k)}$ is the distance between the soft parton with momentum k and the hard parton i, and $i = 3, \ldots, n+2$ runs over the final-state Born jets. We also need to specify the soft limit of the approximation we used in the singular region where the radiation is collinear to an initial-state parton, i.e $r_{C_1,S} = r_{C_2,S} = r^{\mathcal{I}^c}$, and in the singular region where the radiation is collinear to the final-state parton i, i.e.

$$(r_{C_i,S})^2 = \frac{(k_{T,C_iS}^{\rm ness})^2}{Q^2} = \frac{k^0}{p_i^0}\frac{2p_i\cdot k}{Q^2D^2}\,, \tag{3.29}$$

where p_i is the four-momentum of the Born-level jet i.

By exploiting the parametrisation outlined in section 2.4, the soft-subtracted contribution in eq. (2.38) can be written in terms of the soft function in eq. (2.39). The soft subtracted current $\mathbf{J}^2_{\rm sub}$ in eq. (2.40) becomes

$$\begin{aligned}\mathbf{J}^2_{\rm sub} = \left(-\mathbf{T}_1\cdot\mathbf{T}_2\omega_{12} - \sum_i(\mathbf{T}_1\cdot\mathbf{T}_i\omega_{1i} + (1\leftrightarrow 2)) - \sum_{i>j}\mathbf{T}_i\cdot\mathbf{T}_j\omega_{ij}\right)\Theta(r_{\rm cut} - r_S)\\ - \left(\mathbf{T}_1^2\omega_2^1 + (1\leftrightarrow 2)\right)\Theta(r_{\rm cut} - r^{\mathcal{I}^c}) - \sum_i \mathbf{T}_i^2\omega_{C_i,S}\Theta(r_{\rm cut} - r_{C_i,S})\,.\end{aligned} \tag{3.30}$$

An analytical closed form for $\mathbf{S}$ is hard to obtain in this case. However, we can analytically extract the ϵ-poles and logarithms of $r_{\rm cut}$. In order to achieve this goal, we reorganise the subtracted current as follows

$$\mathbf{J}^2_{\rm sub} = \mathbf{J}^2_{\rm sing} + (\mathbf{J}^2_{\rm sub} - \mathbf{J}^2_{\rm sing}) \equiv \mathbf{J}^2_{\rm sing} + \mathbf{J}^2_{\rm fin} \tag{3.31}$$

where $\mathbf{J}^2_{\rm sing}$ is still singular in the soft wide-angle limit, whereas

$$\mathbf{S}_{\rm fin} \equiv 2\mu_R^{2\epsilon}\frac{e^{\gamma_E\epsilon}}{\Gamma(1-\epsilon)}\int\frac{d^dk}{\Omega_{d-2}}\delta_+(k^2)\mathbf{J}^2_{\rm fin} \tag{3.32}$$

is finite in $d = 4$ dimensions and can be computed numerically.

JHEP12(2023)193

The soft-singular term $\mathbf{J}^2_{\text{sing}}$ can be defined as

$$\mathbf{J}^2_{\text{sing}} = \sum_i \mathbf{T}_1 \cdot \mathbf{T}_i \Big((\omega_2^1 - \omega_i^1)\Theta(r_{\text{cut}} - k_t/Q) + (\omega_{C_i,S} - \omega_1^i)\Theta(D r_{\text{cut}} - k_{i\perp}/Q) \Big) + (1 \leftrightarrow 2) + \sum_{i\neq j} \mathbf{T}_i \cdot \mathbf{T}_j (\omega_{C_i,S} - \omega_j^i)\Theta(D r_{\text{cut}} - k_{i\perp}/Q) \tag{3.33}$$

where the sum runs over the labels of the final-state partons and $k_{i\perp}$ is the transverse momentum of k with respect to the i-jet direction, in the partonic CM frame, (see appendix C for more details). Note that we split the eikonal terms according to $\omega_{\alpha\beta} = \omega_\beta^\alpha + \omega_\alpha^\beta$ in order to obtain terms which are separately free of collinear divergences. The integral of the singular part

$$\mathbf{S}_{\text{sing}} \equiv 2\mu_R^{2\epsilon} \frac{e^{\gamma_E \epsilon}}{\Gamma(1-\epsilon)} \int \frac{d^d k}{\Omega_{d-2}} \delta_+(k^2) \mathbf{J}^2_{\text{sing}} \tag{3.34}$$

can be related to integrals that are already known from q_T-resummation for heavy-quark production (see appendix C). The final result can be written as

$$\begin{aligned}
\mathbf{S}_{\text{sing}} = \left(\frac{\mu_R^2}{Q^2}\right)^\epsilon \frac{e^{\gamma_E\epsilon}}{\Gamma(1-\epsilon)} \frac{r_{\text{cut}}^{-2\epsilon}}{\epsilon} \Bigg\{ & \sum_i C_{a_i} \log\left(\frac{2E_{J_i}}{Q}\right) + \frac{1}{2}\sum_{\alpha\neq\beta} \log\left(\frac{2p_\alpha\cdot p_\beta}{Q^2}\right) \mathbf{T}_\alpha \cdot \mathbf{T}_\beta \Bigg\} \\
& - \frac{1}{2}\Bigg\{ 2\log(D) \left[\sum_{\alpha\neq\beta} \mathbf{T}_\alpha \cdot \mathbf{T}_\beta \log\left(\frac{2p_\alpha\cdot p_\beta}{Q^2}\right) + 2\sum_i C_{a_i} \log\left(\frac{2E_{J_i}}{Q}\right) \right] \\
& + \sum_i \left[\mathbf{T}_1 \cdot \mathbf{T}_i \left(\text{Li}_2\left(-\frac{2p_2\cdot p_i}{Q^2}\right) + \text{Li}_2\left(-\frac{p_2\cdot p_i}{2E_{J_i}^2}\right)\right) + (1\leftrightarrow 2)\right] \\
& + \sum_{i\neq j} \mathbf{T}_i\cdot\mathbf{T}_j \text{Li}_2\left(-\frac{E_{J_j}^2}{2(p_i\cdot p_j)}\sin^2\theta_{ij}\right)\Bigg\},
\end{aligned} \tag{3.35}$$

where we recall that

$$\cos\theta_{ij} = 1 - \frac{p_i\cdot p_j}{E_{J_i}E_{J_j}}, \qquad E_{J_i} = \frac{p_i\cdot(p_1+p_2)}{Q}. \tag{3.36}$$

We point out that the logarithmic dependence on the jet energies E_{J_i} cancels against the respective terms in the jet functions.

3.2.4 Subtraction coefficients for k_T^{ness} slicing

By adding all contributions we computed in the previous sections, and including the factorisation counterterm in eq. (2.52), the IR singular poles cancel out and we can extract the expression for the $\mathbf{\Sigma}^{1k}$ functions introduced in eq. (2.6):

$$\mathbf{\Sigma}^{12}_{\mathcal{A}b_1b_2}(z_1,z_2) = -\delta_{a_1b_1}\delta_{a_2b_2}\delta(1-z_1)\delta(1-z_2)\Big(C_{a_1}+C_{a_2}+\sum_{a\in\{a_i\}} C_a\Big)\mathbf{1} \tag{3.37}$$

$$\begin{aligned}
\mathbf{\Sigma}^{11}_{\mathcal{A}b_1b_2}(z_1,z_2) = {} & 2\Big(P_{a_1b_1}(z_1;\epsilon=0)\delta_{a_2b_2}\delta(1-z_2) + (1\leftrightarrow 2)\Big)\mathbf{1} \\
& + \delta_{a_1b_1}\delta_{a_2b_2}\delta(1-z_1)\delta(1-z_2)\Bigg\{-2\Big(\gamma_{a_1}+\gamma_{a_2}+\sum_{a\in\{a_i\}}\gamma_a\Big)\mathbf{1} \\
& - 2\log(D)\sum_{a\in\{a_i\}} C_a\mathbf{1} - \sum_{\alpha\neq\beta}\log\left(\frac{2p_\alpha\cdot p_\beta}{Q^2}\right)\mathbf{T}_\alpha\cdot\mathbf{T}_\beta\Bigg\}
\end{aligned} \tag{3.38}$$

JHEP12(2023)193

$$
\begin{aligned}
\mathbf{\Sigma}^{10}_{\mathcal{A}b_1b_2}(z_1,z_2) = {} & \log\left(\frac{Q^2}{\mu_F^2}\right)\Big(P_{a_1b_1}(z_1;\epsilon=0)\delta_{a_2b_2}\delta(1-z_2)+(1\leftrightarrow 2)\Big)\mathbf{1} \\
& + \Big(C_{a_1b_1}(z_1)\delta_{a_2b_2}\delta(1-z_2)+(1\leftrightarrow 2)\Big)\mathbf{1} \\
& + \delta_{a_1b_1}\delta_{a_2b_2}\delta(1-z_1)\delta(1-z_2)\Big\{\Big(H^{(1)}-p_B\beta_0\log\left(\frac{Q^2}{\mu_R^2}\right)\Big)\mathbf{1} \\
& + \sum_{a\in\{a_i\}}\Big(-C_a\log^2 D-2\gamma_a\log(2D)+\kappa_a\Big)\mathbf{1} \\
& - \log(D)\sum_{\alpha\neq\beta}\mathbf{T}_\alpha\cdot\mathbf{T}_\beta\log\left(\frac{2p_\alpha\cdot p_\beta}{Q^2}\right) \\
& - \frac{1}{2}\sum_i\left[\mathbf{T}_1\cdot\mathbf{T}_i\Big(\mathrm{Li}_2\Big(-\frac{2p_2\cdot p_i}{Q^2}\Big)+\mathrm{Li}_2\Big(-\frac{p_2\cdot p_i}{2E_{J_i}^2}\Big)\Big)+(1\leftrightarrow 2)\right] \\
& - \frac{1}{2}\sum_{i\neq j}\mathbf{T}_i\cdot\mathbf{T}_j\mathrm{Li}_2\Big(-\frac{E_{J_j}^2}{2(p_i\cdot p_j)}\sin^2\theta_{ij}\Big)+\mathbf{S}_{\text{fin}}\Big\}\,,
\end{aligned}
\tag{3.39}
$$

where p_B denotes the power of $\alpha_S(\mu_R)$ that appears in the LO cross section. Contrary to what happens for ΔE_t, the coefficient of the double logarithm in r_{cut} is the same for both initial-state and final-state emitters, because k_T^{ness} scales as $\sim E\theta$ in all soft-collinear limits.

3.3 Numerical results

In this section we present some numerical results obtained using ΔE_t and k_T^{ness} as slicing variables. We start by considering Higgs (H) boson production through gluon fusion in association with a jet at the LHC with a CM energy of 13 TeV. We use the `PDF4LHC15_nnlo_30` PDFs [87] with $\alpha_S(m_Z)=0.118$ through the LHAPDF interface [88]. We define jets via the anti-k_T clustering algorithm [89] with $R=0.4$ and $p_T^j>30\,\text{GeV}$. The factorisation (μ_F) and renormalisation (μ_R) scales are set to the Higgs boson mass $m_H=125\,\text{GeV}$.

We compute the corresponding cross section (in the infinite top-mass limit) using both ΔE_t and k_T^{ness} as resolution variables. The k_T^{ness} calculation is carried out within the MATRIX framework [5], using tree-level and one-loop amplitudes evaluated with OPENLOOPS [90–92]. The ΔE_t calculation is implemented in a dedicated code, which uses amplitudes computed with RECOLA [93–95]. To compare the results obtained with a ΔE_t cut against those obtained with k_T^{ness}, we define the minimum r_{cut} on the dimensionless variable $r=\Delta E_t/\sqrt{m_H^2+(p_T^j)^2}$ and $r=k_T^{\text{ness}}/\sqrt{m_H^2+(p_T^j)^2}$ respectively.[7] In figure 1 we study the behaviour of the NLO correction $\Delta\sigma$ as a function of r_{cut} for the ΔE_t and k_T^{ness} calculations, normalised to the result obtained with Catani-Seymour (CS) dipole subtraction [60, 61] (which is independent of r_{cut}) by using MATRIX. Both calculations nicely converge to the expected result as $r_{\text{cut}}\to 0$, but the r_{cut} dependence is very different for the two calculations. The r_{cut} dependence in the case of ΔE_t is rather strong and consistent with a logarithmically enhanced linear behaviour.

[7] In comparing resolution variables having different scalings in the soft-collinear limits, it is possible to assign an exponent $p_X\neq 1$ to the definition of the dimensionless variable $r_X=(X/Q)^{p_X}$ associated with the resolution variable X [9]. In the case of ΔE_t the choice of p_X would be non-trivial as this observable scales differently in the initial- and final-state regions.

JHEP12(2023)193

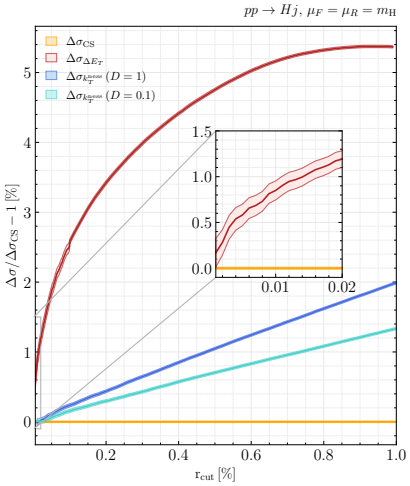

Figure 1. The NLO correction $\Delta\sigma$ to the $H+$ jet cross section computed with ΔE_t (red curve) and k_T^{ness} (blue curves) as function of r_{cut} compared to the r_{cut}-independent result obtained with CS subtraction using MATRIX (orange). In the case of k_T^{ness}, predictions for two different values of the parameter D, $D = 1$ (dark-blue curve) and $D = 0.1$ (light-blue curve), are shown.

By contrast, in the case of k_T^{ness} the dependence is rather mild and linear for both values of D. We observe that k_T^{ness} slicing reaches 1% accuracy at $r_{\text{cut}} = 0.6\%$ ($r_{\text{cut}} = 0.5\%$) for $D = 0.1$ ($D = 1$) while ΔE_t slicing reaches the same accuracy at $r_{\text{cut}} = 0.01\%$.

In figure 2 we show three relevant differential distributions, namely the invariant mass of the $H + 1$ jet system, m_{Hj} (left), the Higgs transverse momentum, $p_{T,H}$ (centre) and the rapidity of the leading jet, y_{j1} (right). Each plot consists of three panels: in the upper panel we display the NLO differential cross section obtained with ΔE_t, k_T^{ness} and CS subtraction; in the central panel we show the ratio between the NLO correction obtained with a slicing method (ΔE_t in red, k_T^{ness} in blue) and the NLO correction computed with CS subtraction (orange); in the lower panel we plot the NLO K-factor K_{NLO}, defined as the ratio of the NLO to the LO distribution. From the central panels we can observe a nice agreement between the results obtained with a slicing method and those computed with CS subtraction. For the m_{Hj} and $p_{T,H}$ distributions the relative differences are around 1% in the bulk region and below 2.5% in the tails where the statistics is much lower and we still experience numerical fluctuations. Concerning the y_{j1} distribution we observe an excellent control over the full rapidity range with differences smaller than 1%.

We also notice that the Higgs p_T distribution displays a perturbative instability at $p_{T,H} = 30\,\text{GeV}$ which corresponds to the cut on the leading jet p_T. This behaviour is not physical but it is expected from a fixed-order computation: even if the observable is IR safe, an integrable divergence arises at a critical point inside the physical region where the distribution is not smooth. This divergence is associated with configurations where the Higgs boson is produced back-to-back to the leading jet in the transverse plane and the additional radiation can only be collinear to the beams or soft. The physical behaviour is restored when the all-order resummation of soft gluons is performed [96].

The k_T^{ness} variable can be also used to evaluate multijet cross sections at NLO accuracy. Results for $Z + 2$ jet processes were presented in ref. [71]. Here we consider trijet production

JHEP12(2023)193

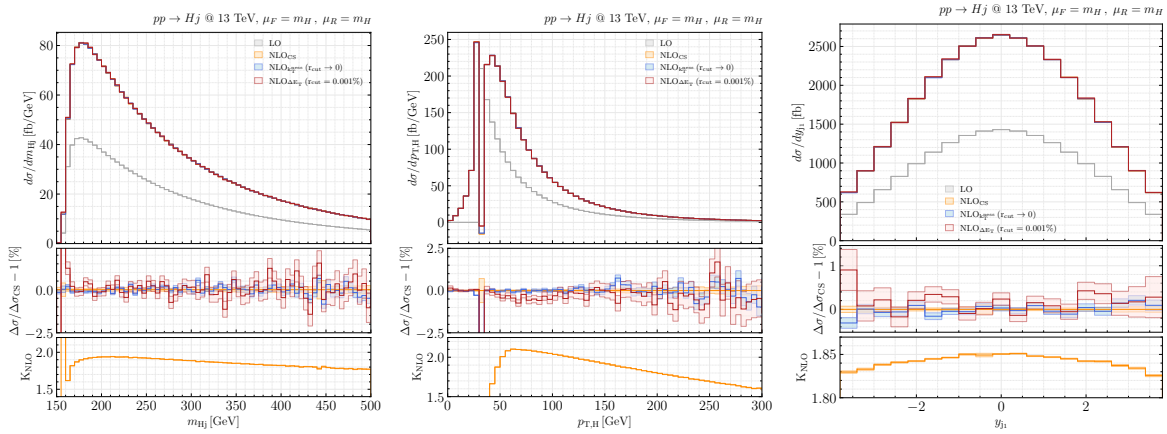

Figure 2. LO and NLO predictions for the invariant mass distribution of the $H+1$ jet system (left), the p_T distribution of the Higgs boson (centre) and the rapidity distribution of the leading jet (right). The NLO correction is computed with ΔE_t, k_T^{ness} and CS subtraction. In the case of ΔE_t, the results are obtained at a fixed $r_{\text{cut}} = 0.001\%$, while, in the case of k_T^{ness}, they are obtained by performing a linear extrapolation to $r_{\text{cut}} \to 0$. For each distribution, absolute predictions are shown in the upper panel, ratios of the NLO correction computed with slicing approaches to the one computed with CS subtraction in the middle panel, and NLO K-factors in the lower panel.

at the LHC with a CM energy of 13 TeV. We use the `NNPDF31_nnlo_as_0118` PDFs [97] and we require three jets in the final state with $p_T^j > 30\,\text{GeV}$ and $|\eta|^j < 4.5$. The factorisation and renormalisation scales are set to the Z-boson mass $m_Z = 91.1876\,\text{GeV}$. We compute the corresponding cross section using k_T^{ness} as resolution variable (with $D = 0.8$) and we define the minimum r_{cut} on the dimensionless variable $r = k_T^{\text{ness}}/m_{jjj}$ where m_{jjj} is the invariant mass of the trijet system.

In figure 3 we study the behaviour of the NLO correction $\Delta\sigma$ as a function of r_{cut} for the k_T^{ness} calculation, normalised to the result obtained with CS dipole subtraction (which is independent of r_{cut}). We can clearly notice that the k_T^{ness} slicing method nicely converges to the expected result and the r_{cut} dependence is purely linear. Compared to the case of H+jet production, the missing power corrections in r_{cut} are much more pronounced (roughly a factor 30 larger) and at $r_{\text{cut}} = 0.2\%$ we are still about 15% away from the exact result. We note however that, since the processes belong to different classes and involve different partonic channels at the Born level, it is not immediate to draw conclusions about the behaviour of the power corrections with respect to the number of jets. Moreover, the hard scale used to normalise k_T^{ness} in figure 1 is not the same as the one in figure 3 and the NLO K-factor for H+jet is roughly a factor four larger than the one for trijet production. If we had used the invariant mass of the Born-like system to define the dimensionless variable r for H+jet, as we do in trijet production, and normalised the missing power corrections to the respective LO cross sections, the slope of the linear power corrections would only have differed by a factor four. In general, the quantitative impact of the linear power corrections may depend both on the hard scale appearing in the definition of the dimensionless variable r and on the parameter D in the k_T^{ness} definition. In the case of H+jet production we have seen in figure 1 that reducing the parameter D from $D = 1$ to $D = 0.1$ reduces the impact of

JHEP12(2023)193

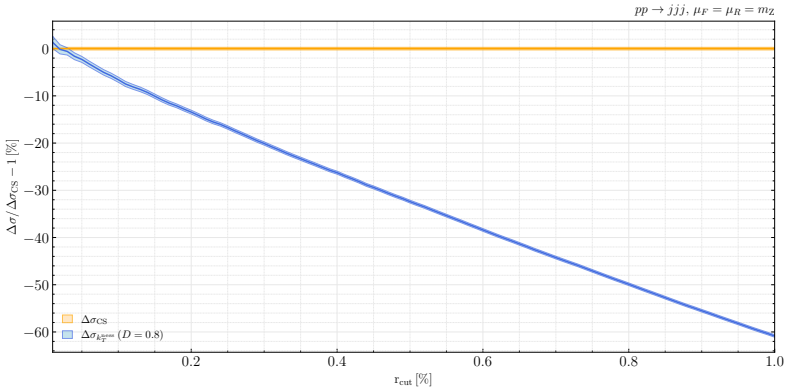

Figure 3. The NLO correction $\Delta\sigma$ to the trijet cross section computed with $k_T^{\rm ness}$ (blue curve) as function of $r_{\rm cut}$ compared to the $r_{\rm cut}$-independent result obtained with dipole subtraction (orange curve).

power corrections in a significant way. In the case of trijet production we find instead that a reduction of D from $D = 0.8$ to $D = 0.1$ leads to a marginal increase of the effect. More detailed studies on these issues are left for future work.

4 Summary

Slicing methods have provided very efficient ways to obtain higher order QCD predictions for a number of benchmark hadron collider processes. These methods are based on identifying a resolution variable to distinguish configurations in which at least one additional QCD parton is resolved. The exploration of new resolution variables can have interesting implications, both in the context of fixed-order calculations, resummed computations and in Monte Carlo event generators.

In this paper we have considered a general class of hadron collider processes: the production of an arbitrary number of jets, possibly accompanied by a colourless system. We have provided a general formulation of a slicing scheme for this class of processes, by identifying the various contributions that need to be computed at NLO. Following the nomenclature customarily used in SCET, these contributions are the parton level beam, jet and soft functions describing initial-state collinear, final-state collinear, and soft wide-angle radiation.

We then focused on two new observables, the one-jet resolution variable ΔE_t and the n-jet resolution variable $k_T^{\rm ness}$ [71], and we have explicitly computed all the perturbative contributions needed to carry out NLO calculations by using these variables. We have shown that the ΔE_t variable, though potentially interesting for one-jet processes, has a non-trivial structure of azimuthal correlations that lead to complications in the evaluation of the beam and jet functions already at NLO. We have presented numerical results for H+jet production using ΔE_t and $k_T^{\rm ness}$, showing the different power suppressed contributions affecting the two variables. While power corrections for $k_T^{\rm ness}$ are purely linear, in the case of ΔE_t they are logarithmically enhanced. We have also shown results for differential distributions obtained with the two slicing methods, and we have presented new results for three jet production obtained with $k_T^{\rm ness}$. Work on the extension of the $k_T^{\rm ness}$ formalism to NNLO is ongoing, and will be reported elsewhere.

JHEP12(2023)193

In a series of appendices we provide extensive details of our calculations. We also computed the jet function for ΔE_t and k_T^{ness} by using alternative SCET-like definitions, which might be more suitable for an extension to NNLO.

Acknowledgments

This work is supported in part by the Swiss National Science Foundation (SNSF) under contracts 200020_188464 and PZ00P2_201878 and by the UZH Forschungskredit Grant FK-22-099. We would like to thank Stefano Catani for helpful discussions. We are grateful to Stefan Kallweit for his support in the implementation of k_T^{ness} in MATRIX and for comments on the manuscript.

A Azimuthal integrals for ΔE_t

When we consider ΔE_t as a resolution variable, both initial- and final-state collinear limits feature a non-trivial dependence on the azimuthal angle in the plane transverse to the collinear direction. In this appendix we will explain related complications that appear in the calculation of the $\mathcal{I}_*$-functions defined in eqs. (2.21) and (2.36) for initial-state and final-state collinear limits, respectively.

In order to treat both collinear limits at the same time, we introduce the notation

$$\Phi \equiv \begin{cases} \phi \\ \varphi \end{cases} \qquad x \equiv \begin{cases} z \\ \xi \end{cases} \qquad k_T \equiv \begin{cases} k_t \\ k_\perp \end{cases} \qquad \mathcal{P}^{\mu\nu}_{(*)} \equiv \begin{cases} P^{\mu\nu}_{(*)}(z, \hat{k}_t; \epsilon) & \text{for ISC} \\ \hat{P}^{\mu\nu}_{(*)}(\xi, \hat{k}_\perp; \epsilon) & \text{for FSC} \end{cases}, \tag{A.1}$$

where $(*)$ stands for an arbitrary splitting. In the initial-state collinear limit (ISC) where a parton splits into a gluon entering the hard process, the corresponding splitting kernel contains a spin-dependent term $\hat{k}_T^\mu \hat{k}_T^\nu$ which is a function of the azimuthal angle Φ. A similar situation occurs in the final-state collinear limit (FSC) when a gluon splits into two collinear partons. If the resolution variable is independent of the azimuthal angle, one can straightforwardly perform the azimuthal integrals in eqs. (2.22) and (2.37)

$$\int \frac{d\Omega_{d-2}}{\Omega_{d-2}} \mathcal{P}^{\mu\nu}_{(*)}(x, \hat{k}_T; \epsilon) = \mathcal{P}_{(*)}(x; \epsilon)(-g^{\mu\nu}) \,. \tag{A.2}$$

This corresponds to replacing the spin-polarised splitting kernel $\mathcal{P}^{\mu\nu}_{(*)}(x, \hat{k}_T; \epsilon)$ with the averaged one $\mathcal{P}_{(*)}(x; \epsilon)$ in the approximation of the matrix element and using the fact that

$$-g_{\mu\nu} \mathcal{T}^{\mu\nu}_{\mathcal{A}} = |\mathcal{M}^{(0)}_{\mathcal{A}}|^2 \,, \tag{A.3}$$

where $\mathcal{A}$ is the multi-index labelling a Born channel.

In the general case, the splitting kernel can be decomposed as the sum of a spin-averaged part $\mathcal{P}_{(*)}$ and a contribution proportional to $G_{(*)}$ that averages to zero when the slicing variable has a trivial dependence on the azimuthal angle, namely

$$\mathcal{P}^{\mu\nu}_{(*)}(x, \hat{k}_T; \epsilon) = \mathcal{P}_{(*)}(x; \epsilon)(-g^{\mu\nu}) - G_{(*)}(x) \left(-g^{\mu\nu} - 2(1-\epsilon) \hat{k}_T^\mu \hat{k}_T^\nu \right) , \tag{A.4}$$

JHEP12(2023)193

where $\hat{k}_T^\mu = \frac{k_T^\mu}{|\vec{k}_T|}$ is the normalised transverse four-momentum. All $\mathcal{P}_{(*)}$ and $G_{(*)}$ functions are listed in appendix B. If we plug eq. (A.4) in the expression of the $\mathcal{I}_*$ integrals in eqs. (2.21) and (2.36), we end up with two contributions for the spin-averaged and spin-dependent parts, respectively. The azimuthal dependence of the slicing variable does not significantly increase the complexity of the spin-averaged integral, thus we will focus on the spin dependent part in the following.

We can first perform the integration over all radiation variables except the angular dependence in the transverse plane $d\Omega_{d-2}$. By dropping power corrections in the slicing parameter, r_{cut}, we arrive at integrals of type

$$\mathcal{I}_\Phi^{\mu\nu} = \int \frac{d\Omega_{d-3}}{\Omega_{d-2}} \int_0^\pi d\Phi (\sin\Phi)^{-2\epsilon}\, g(\Phi) \left(-g^{\mu\nu} - 2(1-\epsilon)\hat{k}_T^\mu \hat{k}_T^\nu\right) \tag{A.5}$$

to be contracted with the spin-polarised tensor $\mathcal{T}_\mathcal{A}^{\mu\nu}$. The function $g(\Phi)$ embodies the remaining dependence on Φ after the integration over the transverse momentum: in the initial-state collinear limit we find $g(\phi) = (1+\cos\phi)^{2\epsilon}$, while in the final-state collinear limit we have $g(\varphi) = (\sin\varphi)^{2\epsilon}$. In order to perform the integral of $\hat{k}_T^\mu \hat{k}_T^\nu$, we remind the reader that $\cos\phi = \frac{\vec{p}_{F,t}\cdot\vec{k}_t}{p_{F,t}k_t}$ for the initial-state collinear limit and $\cos\varphi = \frac{\vec{p}_{1,\perp}\cdot\vec{k}_\perp}{p_{1,\perp}k_\perp}$ for the final-state collinear limit. Then, we can write the transverse unit vector as

$$\hat{k}_T^\mu = \cos\Phi\, \mathcal{E}_1^\mu + \sin\Phi\, \mathcal{E}_2^\mu(\Omega_{d-3})\,, \tag{A.6}$$

where we defined

$$\mathcal{E}_1^\mu = \begin{cases} \epsilon_1^\mu = \frac{p_{F,t}^\mu}{|\vec{p}_{F,t}|} & \text{for ISC} \\ \varepsilon_1^\mu = \frac{p_{1,\perp}^\mu}{|\vec{p}_{1,\perp}|} & \text{for FSC}\,, \end{cases} \tag{A.7}$$

while $\mathcal{E}_2^\mu(\Omega_{d-3})$ lives on the unit sphere of the $(d-3)$-dimensional space orthogonal to $\mathcal{E}_1^\mu$. The four-vectors $\mathcal{E}_1^\mu$ and $\mathcal{E}_2^\mu$ satisfy the conditions $\mathcal{E}_1^2 = \mathcal{E}_2^2 = -1$ and $\mathcal{E}_1 \cdot \mathcal{E}_2 = 0$. It follows that

$$\begin{aligned} -2(1-\epsilon)\int \frac{d\Omega_{d-2}}{\Omega_{d-2}} g(\Phi)\, \hat{k}_T^\mu \hat{k}_T^\nu = -\frac{2(1-\epsilon)}{\Omega_{d-2}} \int_0^\pi d\Phi (\sin\Phi)^{-2\epsilon} g(\Phi) \int d\Omega_{d-3} \\ \times \left(\cos^2\Phi \mathcal{E}_1{}^\mu \mathcal{E}_1{}^\nu + \sin\Phi\cos\Phi\,(\mathcal{E}_1{}^\mu \mathcal{E}_2{}^\nu + \mathcal{E}_2{}^\mu \mathcal{E}_1{}^\nu) + \sin^2\Phi \mathcal{E}_2{}^\mu \mathcal{E}_2{}^\nu\right). \end{aligned} \tag{A.8}$$

The integral of $\sin\Phi\cos\Phi\,(\mathcal{E}_1{}^\mu\mathcal{E}_2{}^\nu + \mathcal{E}_2{}^\mu\mathcal{E}_1{}^\nu)$ vanishes because the integrand is anti-symmetric in the $(d-3)$-dimensional subspace. The only non-trivial contribution to the $d\Omega_{d-3}$-integral is

$$\int d\Omega_{d-3} \mathcal{E}_2{}^\mu \mathcal{E}_2{}^\nu \sim \frac{\Omega_{d-3}}{d-3}\left(-g^{\mu\nu} - \mathcal{E}_1^\mu \mathcal{E}_1^\nu\right), \tag{A.9}$$

where $\sim$ means that we are dropping terms which are vanishing when contracted with the $\mathcal{T}_\mathcal{A}^{\mu\nu}$ tensor, due to gauge invariance. Taking into account the previous considerations, we can rewrite $\mathcal{I}_\Phi^{\mu\nu}$ as

$$\begin{aligned} \mathcal{I}_\Phi^{\mu\nu} &= \frac{\Omega_{d-3}}{\Omega_{d-2}} \int_0^\pi d\Phi (\sin\Phi)^{-2\epsilon} g(\Phi) \left(-g^{\mu\nu} - 2(1-\epsilon)\cos^2\Phi\, \mathcal{E}_1{}^\mu \mathcal{E}_1{}^\nu - \frac{2-2\epsilon}{1-2\epsilon}\sin^2\Phi\,(-g^{\mu\nu} - \mathcal{E}_1^\mu \mathcal{E}_1^\nu)\right) \\ &= \frac{\Omega_{d-3}}{\Omega_{d-2}} \int_0^\pi d\Phi (\sin\Phi)^{-2\epsilon}\, g(\Phi) \left(\cos^2\Phi - \frac{\sin^2\Phi}{1-2\epsilon}\right)\left((-g^{\mu\nu} + \mathcal{A}^{\mu\nu})\epsilon - \mathcal{A}^{\mu\nu}\right) \end{aligned} \tag{A.10}$$

JHEP12(2023)193

where we introduced the asymmetry tensor $\mathcal{A}^{\mu\nu} = 2\mathcal{E}_1^\mu \mathcal{E}_1^\nu + g^{\mu\nu}$. It is worth noticing that, if $g(\Phi)$ is constant, the integral $\mathcal{I}_\Phi^{\mu\nu}$ is identically zero to all orders in ϵ.

In the full computation of the initial- and final-state collinear contributions, $\mathcal{I}_\Phi^{\mu\nu}$ multiplies a single $1/\epsilon$ pole and, thus, we need the result up to $\mathcal{O}(\epsilon^2)$, namely

$$\mathcal{I}_\Phi^{\mu\nu} = \begin{cases} -\int_0^\pi \frac{d\phi}{\pi} \left(\frac{1+\cos\phi}{\sin\phi}\right)^{2\epsilon} \left(\cos^2\phi - \frac{\sin^2\phi}{1-2\epsilon}\right) \mathcal{A}^{\mu\nu} + \mathcal{O}(\epsilon^2) = \epsilon \mathcal{A}^{\mu\nu} + \mathcal{O}(\epsilon^2) & \text{for ISC} \\ -\int_0^\pi \frac{d\varphi}{\pi} \left(\cos^2\varphi - \frac{\sin^2\varphi}{1-2\epsilon}\right) \mathcal{A}^{\mu\nu} + \mathcal{O}(\epsilon^2) = \epsilon \mathcal{A}^{\mu\nu} + \mathcal{O}(\epsilon^2) & \text{for FSC} \end{cases} . \tag{A.11}$$

In conclusion, it turns out that the spin-dependent part of the $\mathcal{I}_*$ integrals is proportional to the contraction $\mathcal{A}^{\mu\nu}\mathcal{T}_{\mathcal{A},\mu\nu}$. This quantity can be directly evaluated in $d = 4$ dimensions as

$$\mathcal{A}^{\mu\nu}\mathcal{T}_{\mathcal{A},\mu\nu} = |\mathcal{M}_{\mathcal{A}}^{(0),\mathcal{E}_1}|^2 - |\mathcal{M}_{\mathcal{A}}^{(0),\mathcal{E}_2}|^2 \tag{A.12}$$

where we defined the polarised Born matrix elements as $|\mathcal{M}_{\mathcal{A}}^{(0),\mathcal{E}_i}|^2 = \mathcal{T}_{\mathcal{A},\mu\nu}\mathcal{E}_i^\mu \mathcal{E}_i^\nu$, $i = 1, 2$. Having these results in mind, we can derive the formulæ in eqs. (3.5) and (3.9).

B Splitting kernels

In the initial-state collinear limit, we use the regularised and spin-polarised splitting kernels

$$\begin{aligned} P_{qq}^{ss'}(z, \hat{k}_t; \epsilon) &= P_{qq}(z; \epsilon)\, \delta^{ss'} \\ P_{qg}^{ss'}(z, \hat{k}_t; \epsilon) &= P_{qg}(z; \epsilon)\, \delta^{ss'} \\ P_{gg}^{\mu\nu}(z, \hat{k}_t; \epsilon) &= P_{gg}(z; \epsilon)(-g^{\mu\nu}) - G_{gg}(z)\left(-g^{\mu\nu} - 2(1-\epsilon)\hat{k}_t^\mu \hat{k}_t^\nu\right) \\ P_{gq}^{\mu\nu}(z, \hat{k}_t; \epsilon) &= P_{gq}(z; \epsilon)(-g^{\mu\nu}) - G_{gq}(z)\left(-g^{\mu\nu} - 2(1-\epsilon)\hat{k}_t^\mu \hat{k}_t^\nu\right) \end{aligned} \tag{B.1}$$

where the spin-averaged splitting kernels are

$$\begin{aligned} P_{qq}(z; \epsilon) &= \frac{C_F}{2}\left(\frac{z^2+1}{(1-z)_+} - \epsilon(1-z)\right) + \frac{3}{4} C_F \delta(1-z) \\ P_{qg}(z; \epsilon) &= \frac{T_R}{2}\left(1 - \frac{2z(1-z)}{1-\epsilon}\right) \\ P_{gg}(z; \epsilon) &= C_A\left(\frac{z}{(1-z)_+} + \frac{1-z}{z} + z(1-z)\right) + \beta_0 \delta(1-z) \\ P_{gq}(z; \epsilon) &= \frac{C_F}{2}\left(\frac{(1-z)^2+1}{z} - \epsilon z\right) . \end{aligned} \tag{B.2}$$

One can obtain the unregularised splitting kernels $\hat{P}$ by simply replacing $(1-z)_+ \to (1-z)$ and dropping terms proportional to $\delta(1-z)$. The functions $G_{ab}(z)$ are [98]

$$G_{gg}(z) = C_A \frac{1-z}{z} \qquad\qquad G_{gq}(z) = C_F \frac{1-z}{z} \tag{B.3}$$

JHEP12(2023)193

and the functions $C_{ab}(z)$ read [86]

$$C_{gq}(z) = \frac{C_F}{2} z \qquad C_{qq}(z) = \frac{C_F}{2}(1-z) \qquad C_{qg}(z) = T_R z(1-z)\,. \tag{B.4}$$

In the final-state collinear limit, we use the unregularised and spin-polarised splitting kernels

$$\begin{aligned}
\hat{P}^{ss'}_{q\to qg}(\xi,\hat{k}_\perp;\epsilon) &= \hat{P}_{q\to qg}(\xi;\epsilon)\,\delta^{ss'} = \hat{P}^{ss'}_{q\to gq}(1-\xi,k_\perp;\epsilon)\\
\hat{P}^{\mu\nu}_{g\to gg}(\xi,\hat{k}_\perp;\epsilon) &= \hat{P}_{g\to gg}(\xi;\epsilon)(-g^{\mu\nu}) - G_{g\to gg}(\xi,\epsilon)\Big(-g^{\mu\nu} - 2(1-\epsilon)\hat{k}^\mu_\perp \hat{k}^\nu_\perp\Big)\\
\hat{P}^{\mu\nu'}_{g\to q\bar{q}}(\xi,\hat{k}_\perp;\epsilon) &= \hat{P}_{g\to q\bar{q}}(\xi;\epsilon)(-g^{\mu\nu}) - G_{g\to q\bar{q}}(\xi,\epsilon)\Big(-g^{\mu\nu} - 2(1-\epsilon)\hat{k}^\mu_\perp \hat{k}^\nu_\perp\Big)
\end{aligned} \tag{B.5}$$

where the spin-averaged splitting kernels and the functions $G_{g\to gg}(\xi,\epsilon)$ and $G_{g\to q\bar{q}}(\xi,\epsilon)$ read

$$\begin{aligned}
\hat{P}_{q\to qg}(\xi;\epsilon) &= \frac{C_F}{2}\left(\frac{\xi^2+1}{1-\xi} - \epsilon(1-\xi)\right) = \hat{P}_{q\to gq}(1-\xi;\epsilon)\\
\hat{P}_{g\to gg}(\xi;\epsilon) &= \frac{C_A}{2}\left(\frac{\xi}{1-\xi} + \frac{1-\xi}{\xi} + \xi(1-\xi)\right)\\
\hat{P}_{g\to q\bar{q}}(\xi;\epsilon) &= \frac{T_R}{2}\left(1 - \frac{2\xi(1-\xi)}{1-\epsilon}\right)\\
G_{g\to gg}(\xi,\epsilon) &= \frac{C_A}{2}\xi(1-\xi)\\
G_{g\to q\bar{q}}(\xi,\epsilon) &= -\frac{T_R}{1-\epsilon}\xi(1-\xi)\,.
\end{aligned} \tag{B.6}$$

Note that we already include a symmetry factor 1/2 for the identical gluons in the final-state $g\to gg$ splitting kernels and G functions, i.e., there are no symmetry factors in the phase space.

C Soft integrals for k_T^{ness}

In this appendix we discuss the integration, over the radiation phase space, of the soft singular term $\mathbf{J}^2_{\text{sing}}$ defined in eq. (3.33). We start by noticing that the result is the sum of integrals of the type

$$2\mu_R^{2\epsilon}\frac{e^{\gamma_E\epsilon}}{\Gamma(1-\epsilon)}\int\frac{d^dk}{\Omega_{d-2}}\,\delta_+(k^2)\Theta\left(r_{\text{cut}} - \frac{k_T}{Q}\right)J(k,p;v_1,v_2), \tag{C.1}$$

where the function $J(k,p;v_1,v_2) = \frac{1}{p\cdot k}\left(\frac{p\cdot v_1}{v_1\cdot k} - \frac{p\cdot v_2}{v_2\cdot k}\right)$ is integrated over the radiation phase space d^dk and depends on two massive four-vectors v_i $(i=1,2)$ and a massless four-vector p. Indeed, we can consider eq. (3.33) and easily identify three families of integrals of the type in eq. (C.1) according to the choice of p, v_1 and v_2. The first contribution is

$$\omega_2^1 - \omega_i^1 = \frac{1}{p_1\cdot k}\left(\frac{p_1\cdot(p_1+p_2)}{k\cdot(p_1+p_2)} - \frac{p_1\cdot(p_1+p_i)}{k\cdot(p_1+p_i)}\right) = J(k,p_1;p_1+p_2,p_1+p_i)\,, \tag{C.2}$$

where p_1 and p_2 are initial-state momenta and p_i is the momentum of a final-state parton. The second contribution is of type

$$\omega_{C_i,S} - \omega_1^i = \frac{1}{p_i\cdot k}\left(\frac{p_i\cdot(p_1+p_2)}{k\cdot(p_1+p_2)} - \frac{p_i\cdot(p_i+p_1)}{k\cdot(p_i+p_1)}\right) = J(k,p_i;p_1+p_2,p_i+p_1)\,, \tag{C.3}$$

JHEP12(2023)193

while the last contribution is of type

$$\omega_{C_i,S} - \omega_j^i = \frac{1}{p_i \cdot k}\left(\frac{p_i \cdot (p_1+p_2)}{k \cdot (p_1+p_2)} - \frac{p_i \cdot (p_i+p_j)}{k \cdot (p_i+p_j)}\right) = J(k, p_i; p_1+p_2, p_i+p_j). \tag{C.4}$$

The b-space transformation for the function $J(k,p;v_1,v_2)$ is known from q_T-resummation of heavy-quark pair production and it is given by [80]

$$\begin{aligned}\langle I(\vec{b})\rangle &= \left\langle \int d^dk \delta_+\left(k^2\right) e^{i\vec{k}_T\cdot\vec{b}}\, J(k,p;v_1,v_2)\right\rangle \\ &= \frac{1}{4}\Omega_{d-2}\Gamma^2(1-\epsilon)\left(\frac{b^2}{4}\right)^{\epsilon}\left[-\frac{2}{\epsilon}\ln\left(\frac{p\cdot v_1\sqrt{v_2^2}}{p\cdot v_2\sqrt{v_1^2}}\right)+\mathrm{Li}_2\left(-\frac{v_{1,T}^2}{v_1^2}\right)-\mathrm{Li}_2\left(-\frac{v_{2,T}^2}{v_2^2}\right)+\mathrm{O}(\epsilon)\right],\end{aligned} \tag{C.5}$$

where $b^2 \equiv (\vec{b})^2$, $v_{i,T}^2 \equiv (\vec{v}_{i,T})^2$ and $\langle\cdots\rangle$ stands for the $(d-2)$-dimensional azimuthal average over the direction of the impact parameter $\vec{b}$.

The integral in eq. (C.1) can be related to eq. (C.5) via

$$\begin{aligned}&2\mu_R^{2\epsilon}\frac{e^{\gamma_E\epsilon}}{\Gamma(1-\epsilon)}\int\frac{d^dk}{\Omega_{d-2}}\,\delta_+(k^2)\Theta\left(r_{\mathrm{cut}}-\frac{k_T}{Q}\right)J(k,p;v_1,v_2) = \\ &= \left(\frac{\mu_R^2}{Q^2}\right)^{\epsilon} r_{\mathrm{cut}}^{-2\epsilon}\frac{e^{\gamma_E\epsilon}}{\Gamma(1-\epsilon)}\frac{2\langle I(\vec{b})\rangle}{\Omega_{d-2}\Gamma^2(1-\epsilon)\left(\frac{b^2}{4}\right)^{\epsilon}},\end{aligned} \tag{C.6}$$

where $Q = \sqrt{(p_1+p_2)^2}$ is the invariant mass of the system. The previous relation can be derived by writing the Θ-function in Fourier space as

$$\Theta\left(r_{\mathrm{cut}}-\frac{k_T}{Q}\right) = \int_0^{r_{\mathrm{cut}}Q} d^{d-2}k'_T\,\delta^{(d-2)}(\vec{k}_T-\vec{k}'_T) = \int_0^{r_{\mathrm{cut}}Q} d^{d-2}k'_T\int\frac{d^{d-2}b}{(2\pi)^{d-2}}e^{i(\vec{k}_T-\vec{k}'_T)\cdot\vec{b}} \tag{C.7}$$

and then performing the integral over the $(d-2)$-dimensional azimuthal space around the direction of the impact parameter. The final result for the integral in eq. (C.1) depends on the transverse momenta $v_{i,T}$ with respect to the massless four-vector p. The transverse component v_T of a generic four-vector v can be defined uniquely by introducing a generic reference vector N and by considering the following decomposition:

$$v_T = v - \frac{v\cdot\left(N - p\frac{N^2}{N\cdot p}\right)}{N\cdot p}p - \frac{v\cdot p}{N\cdot p}N\,, \tag{C.8}$$

which satisfies the conditions $p\cdot v_T = N\cdot v_T = 0$. In this paper we implicitly choose $N = p_1+p_2$ such that $\vec{v}_T \equiv \vec{v}_t$ coincides with the transverse momentum with respect to the beam direction if p is an initial-state parton, while $\vec{v}_T \equiv \vec{v}_\perp$ lives in the plane orthogonal to $\vec{p}$ in the Born CM frame (note that in this frame $\vec{p}_1+\vec{p}_2 = \vec{0}$).

Finally, we obtain

$$\begin{aligned}&2\mu_R^{2\epsilon}\frac{e^{\gamma_E\epsilon}}{\Gamma(1-\epsilon)}\int\frac{d^dk}{\Omega_{d-2}}\,\delta_+(k^2)\Theta\left(r_{\mathrm{cut}}-\frac{k_t}{Q}\right)J(k,p_1;p_1+p_2,p_1+p_i) \\ &= \frac{1}{2}\left(\frac{\mu_R^2}{Q^2}\right)^{\epsilon} r_{\mathrm{cut}}^{-2\epsilon}\frac{e^{\gamma_E\epsilon}}{\Gamma(1-\epsilon)}\left\{-\frac{1}{\epsilon}\ln\left(\frac{p_1\cdot p_2}{p_1\cdot p_i}\right)+\mathrm{Li}_2\left(-\frac{p_{i,t}^2}{2p_1\cdot p_i}\right)\right\}+\mathrm{O}(\epsilon),\end{aligned} \tag{C.9}$$

JHEP12(2023)193

$$
\begin{aligned}
&2\mu_R^{2\epsilon}\frac{e^{\gamma_E\epsilon}}{\Gamma(1-\epsilon)}\int\frac{d^dk}{\Omega_{d-2}}\,\delta_+(k^2)\Theta\left(r_{\text{cut}}-\frac{k_\perp}{Q}\right)J(k,p_i;p_1+p_2,p_i+p_1)\\
&=\frac{1}{2}\left(\frac{\mu_R^2}{Q^2}\right)^{\epsilon}r_{\text{cut}}^{-2\epsilon}\frac{e^{\gamma_E\epsilon}}{\Gamma(1-\epsilon)}\left\{-\frac{2}{\epsilon}\ln\left(\frac{p_i\cdot(p_1+p_2)\sqrt{2p_i\cdot p_1}}{p_i\cdot p_1\sqrt{2p_1\cdot p_2}}\right)+\text{Li}_2\left(-\frac{p_{1,\perp}^2}{2p_1\cdot p_i}\right)\right\}+\text{O}(\epsilon)\\
&=\frac{1}{2}\left(\frac{\mu_R^2}{Q^2}\right)^{\epsilon}r_{\text{cut}}^{-2\epsilon}\frac{e^{\gamma_E\epsilon}}{\Gamma(1-\epsilon)}\left\{-\frac{1}{\epsilon}\ln\left(\frac{2E_{J_i}^2}{p_i\cdot p_1}\right)+\text{Li}_2\left(-\frac{p_{1,\perp}^2}{2p_1\cdot p_i}\right)\right\}+\text{O}(\epsilon),
\end{aligned}
\tag{C.10}
$$

$$
\begin{aligned}
&2\mu_R^{2\epsilon}\frac{e^{\gamma_E\epsilon}}{\Gamma(1-\epsilon)}\int\frac{d^dk}{\Omega_{d-2}}\,\delta_+(k^2)\Theta\left(r_{\text{cut}}-\frac{k_\perp}{Q}\right)J(k,p_i;p_1+p_2,p_i+p_j)\\
&=\frac{1}{2}\left(\frac{\mu_R^2}{Q^2}\right)^{\epsilon}r_{\text{cut}}^{-2\epsilon}\frac{e^{\gamma_E\epsilon}}{\Gamma(1-\epsilon)}\left\{-\frac{2}{\epsilon}\ln\left(\frac{p_i\cdot(p_1+p_2)\sqrt{2p_i\cdot p_j}}{p_i\cdot p_j\sqrt{2p_1\cdot p_2}}\right)+\text{Li}_2\left(-\frac{p_{j,\perp}^2}{2p_j\cdot p_i}\right)\right\}+\text{O}(\epsilon)\\
&=\frac{1}{2}\left(\frac{\mu_R^2}{Q^2}\right)^{\epsilon}r_{\text{cut}}^{-2\epsilon}\frac{e^{\gamma_E\epsilon}}{\Gamma(1-\epsilon)}\left\{-\frac{1}{\epsilon}\ln\left(\frac{2E_{J_i}^2}{p_i\cdot p_j}\right)+\text{Li}_2\left(-\frac{p_{j,\perp}^2}{2p_j\cdot p_i}\right)\right\}+\text{O}(\epsilon)\,,
\end{aligned}
\tag{C.11}
$$

for the three families of integrals introduced above.

D SCET-like definition of the NLO jet function

In Section (2.3) we obtained the contribution from the final-state collinear radiation by starting from an exact parametrization of the phase space. Then, we expanded the matrix element and parts of the phase space in the limit where the angle between the two collinear partons becomes small. The advantage of this method is that it yields jet and soft functions with a very clear physical origin. The jet function always contains the collinear singularity as well as the soft-collinear contribution; its definition does not depend on the scaling of the slicing variable in the respective region and, in particular, it is agnostic to whether the slicing variable belongs to the class of SCET_I or SCET_II problems. The (subtracted) soft function is then only related to soft wide-angle radiation.

On the other hand the method outlined in Section (2.3) has the disadvantage that it does not achieve a full separation of scales between the collinear and the soft regions, even in cases where such a separation is possible. To see this, consider the result of eq. (3.9) for the final-state collinear region in the case of ΔE_t-slicing. The result depends non-trivially on the jet energy E_J and on the jet transverse momentum $p_{J,t}$. However, when the final-state collinear region is combined with the soft one in Section (3.1.4), the dependence on E_J drops out, suggesting that it is unphysical and frame dependent. To make the separation of scales more apparent, we can follow a strategy similar to the one exploited in SCET or, in other words, we can exploit the method of regions to give a definition of the jet and soft functions.

In order to identify the different regions, we need to introduce collinear and anti-collinear reference vectors for each (Born level) jet. We find it useful to set up the reference vectors in such a way that the transverse components of the momenta are purely spatial in the partonic CM frame. To this purpose, we introduce a massive reference vector $N = p_1 + p_2$, where p_1 and p_2 are the momenta of the initial-state partons. Having this in mind, for a given (massless) Born level jet with four-momentum p, we can define the collinear and

JHEP12(2023)193

anti-collinear reference vectors

$$n = \frac{\sqrt{N^2}}{p\cdot N}p\,, \qquad \bar{n} = \frac{2}{\sqrt{N^2}}N - n \tag{D.1}$$

satisfying $n^2 = \bar{n}^2 = 0$ and $n\cdot\bar{n} = 2$. Then, we can decompose every four-vector k as

$$k = k^- n + k^+ \bar{n} + k_\perp\,, \tag{D.2}$$

where $k^- = \frac{k\cdot\bar{n}}{2}$ and $k^+ = \frac{k\cdot n}{2}$, and $k_\perp$ is the purely spatial transverse component with $k_\perp\cdot n = k_\perp\cdot\bar{n} = 0$. We also introduce the collinear momentum fraction $z = \frac{k\cdot\bar{n}}{p\cdot\bar{n}} = \frac{k_-}{p_-}$.

We consider the splitting $a_i(\tilde{p}_i)\to a(k) + b(p_i)$. For a generic resolution variable r, we can define the differential NLO jet function as

$$\begin{aligned}
\tilde{j}^{ss'}_{a_i\to ab}(r) &= \frac{\mu_R^{2\epsilon}}{\Omega_{2-2\epsilon}}\frac{e^{\epsilon\gamma_E}}{\Gamma(1-\epsilon)}\frac{\alpha_S(\mu_R)}{\pi}\int\frac{dz_k}{z_k}\int\frac{dz_{p_i}}{z_{p_i}}\int d^{d-2}k_\perp\int d^{d-2}p_{\perp,i}\frac{\hat{P}^{ss'}_{a_i\to ab}(\{k\})}{k\cdot p_i}\\
&\quad\times\delta(z_k + z_{p_i} - 1)\delta^{d-2}(k_\perp + p_{\perp,i})\delta(r - r^{C_i}(\{p_3,\dots,\tilde{p}_i,\dots,p_{n+2}\}))\\
&= \mu_R^{2\epsilon}\frac{e^{\epsilon\gamma_E}}{\Gamma(1-\epsilon)}\frac{\alpha_S(\mu_R)}{\pi}\int\frac{d\Omega_{2-2\epsilon}}{\Omega_{2-2\epsilon}}\int_0^1 dz\int\frac{dk_\perp^2}{(k_\perp^2)^{1+\epsilon}}\hat{P}^{ss'}_{a_i\to ab}(z,\hat{k}_\perp;\epsilon)\delta(r - r^{C_i}(z,k_\perp))\\
&= \left(\frac{\mu_R^2}{Q^2}\right)^{\epsilon}\frac{e^{\epsilon\gamma_E}}{\Gamma(1-\epsilon)}\frac{\alpha_S(\mu_R)}{\pi}\int\frac{d\Omega_{2-2\epsilon}}{\Omega_{2-2\epsilon}}\int_0^1 dz z^{-\epsilon}(1-z)^{-\epsilon}\\
&\quad\times\int dx x^{-1-\epsilon}\hat{P}^{ss'}_{a_i\to ab}(z,\hat{k}_\perp;\epsilon)\delta(r - r^{C_i}(z,x))\,,
\end{aligned} \tag{D.3}$$

where $\hat{P}^{ss'}_{a_i\to ab}$ is the unregularised and spin-polarised splitting kernel (appendix B), r^{C_i} is the approximation of the slicing variable in the collinear region defined above and Q^2 is the squared CM energy. In the last step we have performed the change of variables to the dimensionless invariant mass $x = 2k\cdot p_i/Q^2 = k_\perp^2/(Q^2 z(1-z))$ at fixed z. The cumulant version of the NLO jet function is obtained by integrating the differential jet function up to r_{cut} and summing over all possible splittings of parton a_i

$$\widetilde{\mathcal{J}}^{ss'}_{a_i}(r_{\text{cut}}) = \sum_{(*)}\int_0^{r_{\text{cut}}} dr\,\tilde{j}^{ss'}_{a_i\to(*)}(r)\,, \tag{D.4}$$

where $(*)$ labels an arbitrary splitting.

Thus, the final-state collinear contribution associated with the limit $k\cdot p_i\to 0$ is given by

$$\widetilde{\mathcal{F}}^c_i = \sum_{\mathcal{A}}\int_0^1 dx_1 f_{a_1}(x_1,\mu_F)\int_0^1 dx_2 f_{a_2}(x_2,\mu_F)\int d\Pi^d_n(q;p_F,\{p_j\}_{j=3}^{n+2})\frac{\mathcal{T}^{ss'}_{a_1a_2;\dots a_i\dots}}{2Q^2}\,\widetilde{\mathcal{J}}^{ss'}_{a_i}(r_{\text{cut}}), \tag{D.5}$$

where $q = p_1 + p_2$ and we summed over the possible Born configurations $\mathcal{A} = \{a_1, a_2, \{a_i\}\}$.

By inspecting eq. (D.3), the new definition of the NLO jet function differs from the one in eq. (2.37) by the absence of the phase space factor beyond the strictly collinear limit given in eq. (2.32). Even though it seems that the soft endpoints $z\to 0$ and $z\to 1$ are regulated by the factors $z^{-\epsilon}$ and $(1-z)^{-\epsilon}$ respectively, the integral over the variable x can generate additional z-dependent terms that spoil this regularisation. Therefore, the

JHEP12(2023)193

SCET-like definition leads to the possible appearance of rapidity divergences as expected when applying the method of regions. One way to treat these rapidity divergences is to consistently introduce rapidity regulators [99–105] in the jet, beam and soft functions associated with each singular region. To make contact with the definition given in section 2.3, we consider here a different method inspired by ref. [106].

We modify the jet function of eq. (D.3) by applying the replacement

$$z = \frac{k\cdot\bar{n}}{\tilde{p}_i\cdot\bar{n}} = \frac{k\cdot\bar{n}}{(k+p_i)\cdot\bar{n}} \to z_N = \frac{k\cdot N}{(k+p_i)\cdot N} \tag{D.6}$$

in the argument of the splitting kernel $\hat{P}^{ss'}_{a_i\to ab}(z,\hat{k}_\perp;\epsilon)$. We refer to this procedure as the "z_N-prescription". We observe that the fraction z_N with the choice $N = p_1 + p_2$ coincides with the energy fraction ξ defined in section 2.3. At fixed x, we can express z in terms of z_N as

$$z \simeq \frac{z_N}{1 - Q^2 x/4(\tilde{p}_i^-)^2}\left(1 - \frac{Q^2}{4(\tilde{p}_i^-)^2}\frac{x(1-z_N)}{z_N}\right). \tag{D.7}$$

Performing a change of variables from z to z_N at fixed x, the NLO differential jet function with the z_N-prescription becomes

$$\begin{aligned}
\tilde{J}^{ss'}_{a_i\to ab}(r) &= \left(\frac{\mu_R^2}{Q^2}\right)^\epsilon \frac{e^{\epsilon\gamma_E}}{\Gamma(1-\epsilon)}\frac{\alpha_S(\mu_R)}{\pi}\int\frac{d\Omega_{2-2\epsilon}}{\Omega_{2-2\epsilon}}\int_0^1 dz z^{-\epsilon}(1-z)^{-\epsilon} \\
&\quad\times\int dx x^{-1-\epsilon}\hat{P}^{ss'}_{a_i\to ab}(z_N,\hat{k}_\perp;\epsilon)\delta(r - r^{C_i}(z,x)) \\
&= \left(\frac{\mu_R^2}{Q^2}\right)^\epsilon \frac{e^{\epsilon\gamma_E}}{\Gamma(1-\epsilon)}\frac{\alpha_S(\mu_R)}{\pi}\int\frac{d\Omega_{2-2\epsilon}}{\Omega_{2-2\epsilon}}\int_0^1 dz_N z_N^{-\epsilon}(1-z_N)^{-\epsilon} \\
&\quad\times\int dx x^{-1-\epsilon}\left(1 - \frac{Q^2}{4(\tilde{p}_i^-)^2}\frac{x}{z_N(1-z_N)}\right)^{-\epsilon}\hat{P}^{ss'}_{a_i\to ab}(z_N,\hat{k}_\perp;\epsilon)\delta(r - r_N^{C_i}(z_N,x)),
\end{aligned} \tag{D.8}$$

where we have introduced the notation $r_N^{C_i}(z_N,x) := r^{C_i}(z(z_N,x),x)$. In the final expression of the above equation, we are allowed to identify $\tilde{p}_i^- \approx \tilde{p}_i^0$, where $\tilde{p}_i^0$ is the energy component in the partonic CM frame. The effect of the z_N-prescription is that of reinstating power corrections beyond the strictly collinear limit. More precisely, it allows us to exactly recover the additional phase space factor in eq. (2.34) starting from a careful expansion in the collinear and soft limits. Therefore, the SCET-like jet function regularised with the z_N-prescription is equivalent to the one obtained in section 2.3 up to the precise expression used for the approximation of the observable in the collinear limit, $r_N^{C_i}$. To be concrete, we consider the case of k_T^{ness} and define $\left(k_T^{\text{ness},C_i}(z,x)\right)^2 = Q^2 zx/((1-z)D^2)$, limiting ourselves, for simplicity, to the case $z < 1/2$ (see eq. (3.24)). Then, applying the change of variables in eq. (D.7), we get

$$\begin{aligned}
\left(k_{T,N}^{\text{ness},C_i}(z_N,x)\right)^2 &= \left(k_T^{\text{ness},C_i}(z_N,x)\right)^2 \frac{1 - \frac{Q^2}{4(\tilde{p}_i^-)^2}\frac{x(1-z_N)}{z_N}}{1 - \frac{Q^2}{4(\tilde{p}_i^-)^2}\frac{xz_N}{1-z_N}} \\
&\approx \left(k_T^{\text{ness},C_i}(z_N,x)\right)^2\left(1 - \frac{Q^2}{4(\tilde{p}_i^-)^2}\frac{x(1-2z_N)}{z_N(1-z_N)}\right) \\
&\approx \left(k_T^{\text{ness},C_i}(z_N,x)\right)^2\left(1 - \frac{Q^2}{4(\tilde{p}_i^-)^2}\frac{x}{z_N(1-z_N)}\right).
\end{aligned} \tag{D.9}$$

JHEP12(2023)193

On the other hand, in section 3.2.2, we made the choice $\left(k_{T,N}^{\text{ness},C_i}(z_N,x)\right)^2=\left(k_T^{\text{ness},C_i}(z_N,x)\right)^2$, see eq. (3.24). As we will show explicitly in the following, this does not change the coefficients of the poles in d dimensions nor those of the logarithms of the observable. Only the constant term can be affected. The difference is compensated by the corresponding change in the soft function. Indeed, the modification of the observable in the collinear limit affects also the related subtraction contribution in the definition of the subtracted current in eq. (2.40). More precisely, the soft limit of the SCET-jet function regularised with the z_N-prescription reads

$$\lim_{k^0\to 0}\tilde{j}^{ss'}_{a_i\to ab}(r)=\mu_R^{2\epsilon}\frac{e^{\epsilon\gamma_E}}{\Gamma(1-\epsilon)}\frac{\alpha_{\text{S}}(\mu_R)}{\pi}C_{a_i}\int\frac{d^dk}{\Omega_{d-2}}\delta_+(k^2)\frac{2\tilde{p}_i\cdot N}{(k\cdot\tilde{p}_i)(k\cdot N)}\delta(r-r^{C_iS}(k))\,, \tag{D.10}$$

where C_{a_i} is the colour Casimir of the parton a_i and $r^{C_iS}(k)$ is obtained by first taking the collinear limit and then the limit where k becomes soft, i.e. taking the leading contribution of $r^{C_i}(z,x)$ for $z\to 0$. In the case of k_T^{ness}, this translates into

$$\left(\frac{k_T^{\text{ness},C_iS}}{Q^2}\right)^2=\frac{zx}{D^2}\approx z_N\left(1-\frac{Q^2}{4(\tilde{p}_i^-)^2}\frac{x}{z_N}\right)\frac{x}{D^2}\approx\frac{k^0}{\tilde{p}_i^0}\frac{2k\cdot p_i}{Q^2D^2}\left(1-\frac{k\cdot p_i}{2\tilde{p}_i^0k^0}\right)\,, \tag{D.11}$$

to be compared with eq. (3.29).

To conclude, in this appendix we have seen that a SCET-like definition of the jet function leads to a clean separation of the different scales. On the other hand, if rapidity divergences are present, the jet function becomes dependent on the scheme chosen to regularise them. Moreover, the regularisation procedure will spoil such a simple scale separation. The ensuing scaling violations, however, are typically easy to extract, at least at NLO (see eq. (D.24) below). In the following, we will compute the jet function in the SCET-like formulation for the two resolution variables considered in this paper, namely ΔE_t and k_T^{ness}. We will also directly compare the jet functions obtained applying the z_N-prescription with those computed in section 3.1.2 and section 3.2.2, respectively.

D.1 ΔE_t jet function

In the ΔE_t case, no rapidity divergences arise, and there is in principle no need to use any regularisation procedure. The SCET-like ΔE_t jet function, at the differential level, is given by

$$\begin{aligned}\tilde{j}^{ss'}_{a_i\to ab}(\Delta E_t/Q)&=\left(\frac{\mu_R^2}{Q^2}\right)^{\epsilon}\frac{e^{\epsilon\gamma_E}}{\Gamma(1-\epsilon)}\frac{\alpha_{\text{S}}(\mu_R)}{\pi}\int_0^1dzz^{-\epsilon}(1-z)^{-\epsilon}\int dxx^{-1-\epsilon}\\&\quad\times\int\frac{d\Omega_{2-2\epsilon}}{\Omega_{2-2\epsilon}}\hat{P}^{ss'}_{a_i\to ab}(z,k_\perp;\epsilon)\,\delta\left(\frac{\Delta E_t}{Q}-\frac{Qx\sin^2\phi}{2\tilde{p}_{i,t}}\right)\\&=\frac{\left(\frac{\mu_R^2}{2\Delta E_t\tilde{p}_{i,t}}\right)^{\epsilon}}{\Delta E_t/Q}\frac{e^{\epsilon\gamma_E}}{\Gamma(1-\epsilon)}\frac{\alpha_{\text{S}}(\mu_R)}{\pi}\frac{\Omega_{1-2\epsilon}}{\Omega_{2-2\epsilon}}\int_0^1dzz^{-\epsilon}(1-z)^{-\epsilon}\int_0^\pi d\phi\hat{P}^{ss'}_{a_i\to ab}(z,\hat{k}_\perp;\epsilon)\,,\end{aligned} \tag{D.12}$$

where $\tilde{p}_{i,t}$ is the transverse momentum with respect to the beam direction. In the case of a quark-initiated splitting ($a_i=q$), the corresponding kernel does not contain any dependence

JHEP12(2023)193

on the azimuthal angle ϕ and the quark jet function is

$$\begin{aligned}\tilde{j}_q^{ss'}(\Delta E_t/Q) &= \tilde{j}_{q\to qg}^{ss'}(\Delta E_t/Q) \\ &= \delta_{ss'}\,\frac{\left(\frac{\mu_R^2}{8\Delta E_t\tilde{p}_{i,t}}\right)^{\epsilon}}{\Delta E_t/Q}\,\frac{e^{\epsilon\gamma_E}}{\Gamma(1-\epsilon)}\,\frac{\alpha_{\rm S}(\mu_R)}{\pi}C_F\left[-\frac{1}{\epsilon}-\frac{3}{4}+\epsilon\left(-\frac{7}{4}+\frac{\pi^2}{3}\right)+\mathcal{O}(\epsilon^2)\right]\end{aligned} \tag{D.13}$$

at the differential level and

$$\tilde{\mathcal{J}}_q^{ss'}(r_{\rm cut}) = \delta_{ss'}\left(\frac{\mu_R^2}{Q^2}\right)^{\epsilon}\frac{e^{\epsilon\gamma_E}}{\Gamma(1-\epsilon)}\,\frac{\alpha_{\rm S}(\mu_R)}{\pi}\left(\frac{Q}{8r_{\rm cut}\tilde{p}_{i,t}}\right)^{\epsilon}C_F\left[\frac{1}{\epsilon^2}+\frac{3}{4\epsilon}+\frac{7}{4}-\frac{\pi^2}{3}+\mathcal{O}(\epsilon)\right] \tag{D.14}$$

at the cumulant level. The gluon-initiated ($a_i = g$) splitting kernel contains a residual dependence on the azimuthal angle ϕ due to the polarisation of the parent gluon. By exploiting the technique explained in the appendix A, we can perform the azimuthal integral and obtain

$$\begin{aligned}\tilde{j}_g^{\mu\nu}(\Delta E_t/Q) &= \tilde{j}_{g\to gg}^{\mu\nu}(\Delta E_t/Q)+\tilde{j}_{g\to q\bar{q}}^{\mu\nu}(\Delta E_t/Q) \\ &= \frac{\left(\frac{\mu_R^2}{2\Delta E_t\tilde{p}_{i,t}}\right)^{\epsilon}}{\Delta E_t/Q}\,\frac{e^{\epsilon\gamma_E}}{\Gamma(1-\epsilon)}\,\frac{\alpha_{\rm S}(\mu_R)}{\pi}\,\frac{\pi\Omega_{1-2\epsilon}}{\Omega_{2-2\epsilon}}\int_0^1 dz z^{-\epsilon}(1-z)^{-\epsilon} \\ &\quad\times\left[-g^{\mu\nu}\left(\hat{P}_{g\to gg}(z;\epsilon)+n_f\hat{P}_{g\to q\bar{q}}(z;\epsilon)\right)-\epsilon\mathcal{A}^{\mu\nu}\left(G_{g\to gg}(z)+n_fG_{g\to q\bar{q}}(z)\right)+\mathcal{O}(\epsilon^2)\right].\end{aligned} \tag{D.15}$$

Thus, the gluon jet function is

$$\begin{aligned}\tilde{j}_g^{\mu\nu}(\Delta E_t/Q) = \frac{\left(\frac{\mu_R^2}{8\Delta E_t\tilde{p}_{i,t}}\right)^{\epsilon}}{\Delta E_t/Q}\,\frac{e^{\epsilon\gamma_E}}{\Gamma(1-\epsilon)}\,\frac{\alpha_{\rm S}(\mu_R)}{\pi}\Bigg\{g^{\mu\nu}\left[\frac{C_A}{\epsilon}+\beta_0+C_A\left(\frac{67}{36}-\frac{\pi^2}{3}\right)\epsilon-T_Rn_f\frac{5}{9}\epsilon\right] \\ -\epsilon\mathcal{A}^{\mu\nu}\left[\frac{C_A}{12}-\frac{T_Rn_f}{6}\right]+\mathcal{O}(\epsilon^2)\Bigg\}\end{aligned} \tag{D.16}$$

at the differential level and

$$\begin{aligned}\tilde{\mathcal{J}}_g^{\mu\nu}(r_{\rm cut}) = &\left(\frac{\mu_R^2}{Q^2}\right)^{\epsilon}\frac{e^{\epsilon\gamma_E}}{\Gamma(1-\epsilon)}\,\frac{\alpha_{\rm S}(\mu_R)}{\pi}\left(\frac{Q}{8r_{\rm cut}\tilde{p}_{i,t}}\right)^{\epsilon} \\ &\times\left\{-g^{\mu\nu}\left[\frac{C_A}{\epsilon^2}+\frac{\beta_0}{\epsilon}+C_A\left(\frac{67}{36}-\frac{\pi^2}{3}\right)-T_Rn_f\frac{5}{9}\right]+\mathcal{A}^{\mu\nu}\left[\frac{C_A}{12}-\frac{T_Rn_f}{6}\right]+\mathcal{O}(\epsilon)\right\}\end{aligned} \tag{D.17}$$

at the cumulant level.

We observe that the SCET-like jet function does not contain any dependence on the jet energy E_{J_i}. Comparing with the result obtained in eq. (3.12) we find

$$\begin{aligned}&\mathcal{J}_a^{ss'}(r_{\rm cut})-\tilde{\mathcal{J}}_a^{ss'}(r_{\rm cut}) \\ &= d_a^{ss'}\,C_a\left(\frac{\mu_R^2}{Q^2}\right)^{\epsilon}\frac{e^{\epsilon\gamma_E}}{\Gamma(1-\epsilon)}\,\frac{\alpha_{\rm S}(\mu_R)}{\pi}\left(\frac{Q}{8r_{\rm cut}\tilde{p}_{i,t}}\right)^{\epsilon}\left(\frac{2E_{J_i}}{Q}\right)^{2\epsilon}\left[-\frac{1}{2\epsilon^2}-\frac{\pi^2}{12}+\mathcal{O}(\epsilon)\right].\end{aligned} \tag{D.18}$$

JHEP12(2023)193

We see that the two jet functions differ already in the pole structure: this is due to a different partition of contributions of soft and collinear origin between the jet and the soft function.

Even if it is not strictly necessary, it is instructive to consider the result for the SCET-like jet function when applying the z_N-prescription. Following the previous discussion, we know that this leads to the jet function in eq. (2.37) up to the definition of the observable in the collinear limit. In this case, we have that

$$\Delta E_t^C(z,x,\phi) = \frac{Q^2 x \sin^2\phi}{2\tilde{p}_{i,t}} \underset{z\to z(z_N,x)}{\to} = \Delta E_{t,N}^C(z_N,x) = \Delta E_t^C(z_N,x)\,, \tag{D.19}$$

since $\Delta E_t^C(z,x,\phi)$ does not depend on z. Therefore, in this case the SCET-like jet function regularised with the z_N-prescription coincides exactly with the one defined in the main text. Comparing with the pure SCET-like definition, we have the advantageous feature that the pole structure is observable independent and predictable both in the collinear region and in the pure soft region.[8]

D.2 k_T^{ness} jet function

Since k_T^{ness} behaves as a transverse momentum in every collinear limit, its SCET-like jet function manifests a rapidity divergence, which we regularise with the z_N-prescription. At the differential level, we have

$$\begin{aligned}\tilde{j}^{ss'}_{a_i\to ab}(k_T^{\text{ness}}/Q) = &\left(\frac{\mu_R^2}{Q^2}\right)^{\epsilon}\frac{e^{\epsilon\gamma_E}}{\Gamma(1-\epsilon)}\frac{\alpha_{\text{S}}(\mu_R)}{\pi}\int_0^1 dz z^{-\epsilon}(1-z)^{-\epsilon}\int dx x^{-1-\epsilon}\\ &\times\int\frac{d\Omega_{2-2\epsilon}}{\Omega_{2-2\epsilon}}\hat{P}^{ss'}_{a_i\to ab}(z_N,\hat{k}_\perp;\epsilon)\,\delta\left(\frac{k_T^{\text{ness}}}{Q}-\sqrt{\frac{z(1-z)x}{\max(z,1-z)^2D^2}}\right)\\ &= d^{ss'}_{a_i}\frac{\left(\frac{\mu_R^2}{k_T^{\text{ness}2}D^2}\right)^{\epsilon}}{k_T^{\text{ness}}/Q}\frac{e^{\epsilon\gamma_E}}{\Gamma(1-\epsilon)}\frac{\alpha_{\text{S}}(\mu_R)}{\pi}2\int_0^1 dz\,\max(z,1-z)^{-2\epsilon}\hat{P}_{a_i\to ab}(z_N;\epsilon)\,,\end{aligned} \tag{D.20}$$

where we used the fact that the slicing variable does not contain any azimuthal dependence which allows us to replace the splitting kernel with its azimuthal average. Starting from eq. (D.7), we express z_N as

$$z_N = \frac{z}{1+\frac{Q^2x}{4(\tilde{p}_i^0)^2}}\left(1+\frac{Q^2x}{4(\tilde{p}_i^0)^2}\frac{1-z}{z}\right)\approx z\left(1+\frac{k_T^{\text{ness}2}D^2}{4(\tilde{p}_i^0)^2z^2}\right)\,, \tag{D.21}$$

where the last approximation contains the leading behaviour in the collinear and soft region. At the leading power, we have to perform integrals of the kind

$$I_{z_N} = \int_0^1 dz\frac{f(z;\epsilon)}{z_N}\,, \tag{D.22}$$

[8] A similar implication was noticed in ref. [107] when discussing the consequences of introducing a rapidity regulator for SCET$_{\text{I}}$ problems.

JHEP12(2023)193

where $f(z;\epsilon)$ is finite in the limit $z \to 0$. By performing the following manipulation

$$\begin{aligned} I_{z_N} &= \int_0^1 dz \frac{f(z)-f(0)}{z} \frac{1}{1+\frac{k_T^{\text{ness}\,2} D^2}{4(\tilde{p}_i^0)^2 z^2}} + f(0) \int_0^1 dz \frac{1}{1+\frac{k_T^{\text{ness}\,2} D^2}{4(\tilde{p}_i^0)^2 z^2}} \\ &= \int_0^1 dz \frac{f(z)-f(0)}{z} - \frac{1}{2} \log\left(\frac{k_T^{\text{ness}\,2} D^2}{4(\tilde{p}_i^0)^2}\right) f(0) + \mathcal{O}\left(\frac{k_T^{\text{ness}\,2}}{(\tilde{p}_i^0)^2}\right) \end{aligned} \tag{D.23}$$

we obtain that the net effect of the z_N-prescription is captured by the replacement

$$\frac{1}{z_N} \to \left(\frac{1}{z}\right)_+ - \frac{1}{2} \log\left(\frac{k_T^{\text{ness}\,2} D^2}{4(\tilde{p}_i^0)^2}\right) \delta(z)\,. \tag{D.24}$$

By summing over all possible splittings $a_i \to (*)$, we find that the differential jet functions in the z_N-prescription are

$$\begin{aligned} &\tilde{j}_{a_i}^{ss'}(k_T^{\text{ness}}/Q) = \\ &\sum_{(*)} \tilde{j}_{a_i \to (*)}^{ss'}(k_T^{\text{ness}}/Q) = 2 d_{a_i}^{ss'} \frac{\left(\frac{\mu_R^2}{k_T^{\text{ness}\,2} D^2}\right)^{\epsilon}}{k_T^{\text{ness}}/Q} \frac{e^{\epsilon\gamma_E}}{\Gamma(1-\epsilon)} \frac{\alpha_{\text{S}}(\mu_R)}{\pi} \\ &\times \begin{cases} -\gamma_q(1-2\epsilon\log 2) + C_F\left[-\frac{1}{2}\log\left(\frac{k_T^{\text{ness}\,2} D^2}{4(\tilde{p}_i^0)^2}\right) + \epsilon\left(\frac{\pi^2}{6} - \frac{7}{4}\right)\right] + O(\epsilon^2) & a_i = q \\ -\gamma_g(1-2\epsilon\log 2) + C_A\left[-\frac{1}{2}\log\left(\frac{k_T^{\text{ness}\,2} D^2}{4(\tilde{p}_i^0)^2}\right) + \epsilon\left(\frac{\pi^2}{6} - \frac{131}{72}\right)\right] + n_f T_R \epsilon \frac{17}{36} + O(\epsilon^2) & a_i = g \end{cases} \end{aligned} \tag{D.25}$$

and the cumulant jet functions are

$$\begin{aligned} &\widetilde{\mathcal{J}}_{a_i}^{ss'}(r_{\text{cut}}) = \\ &d_{a_i}^{ss'} \frac{e^{\epsilon\gamma_E}}{\Gamma(1-\epsilon)} \left(\frac{\mu_R^2}{r_{\text{cut}}^2 D^2 Q^2}\right)^{\epsilon} \frac{\alpha_{\text{S}}(\mu_R)}{\pi} \\ &\times \begin{cases} \frac{C_F}{2\epsilon^2} + \frac{\gamma_q + C_F \log\left(\frac{r_{\text{cut}} DQ}{2\tilde{p}_i^0}\right)}{\epsilon} - 2\gamma_q \log 2 + C_F\left(\frac{7}{4} - \frac{\pi^2}{6}\right) + O(\epsilon) & a_i = q \\ \frac{C_A}{2\epsilon^2} + \frac{\gamma_g + C_A \log\left(\frac{r_{\text{cut}} DQ}{2\tilde{p}_i^0}\right)}{\epsilon} - 2\gamma_g \log 2 + C_A\left(\frac{131}{72} - \frac{\pi^2}{6}\right) + n_f T_R \frac{17}{36} + O(\epsilon) & a_i = g\,. \end{cases} \end{aligned} \tag{D.26}$$

By comparing the SCET-like jet functions regularised with the z_N-prescription with the result in eq. (3.27), we find that, up to $\mathcal{O}(\epsilon^0)$, they differ only by the finite contribution

$$\mathcal{J}_{a_i}^{ss'}(r_{\text{cut}}) - \widetilde{\mathcal{J}}_{a_i}^{ss'}(r_{\text{cut}}) = -d_{a_i}^{ss'} C_{a_i} \frac{\alpha_{\text{S}}(\mu_R)}{\pi} \left(\frac{\pi^2}{12} + O(\epsilon)\right). \tag{D.27}$$

JHEP12(2023)193

References

[1] G. Heinrich, *Collider Physics at the Precision Frontier*, *Phys. Rept.* **922** (2021) 1 [arXiv:2009.00516] [INSPIRE].

[2] A. Huss, J. Huston, S. Jones and M. Pellen, *Les Houches 2021 — physics at TeV colliders: report on the standard model precision wishlist*, *J. Phys. G* **50** (2023) 043001 [arXiv:2207.02122] [INSPIRE].

[3] W.J. Torres Bobadilla et al., *May the four be with you: Novel IR-subtraction methods to tackle NNLO calculations*, *Eur. Phys. J. C* **81** (2021) 250 [arXiv:2012.02567] [INSPIRE].

[4] R. Gavin, Y. Li, F. Petriello and S. Quackenbush, *FEWZ 2.0: A code for hadronic Z production at next-to-next-to-leading order*, *Comput. Phys. Commun.* **182** (2011) 2388 [arXiv:1011.3540] [INSPIRE].

[5] M. Grazzini, S. Kallweit and M. Wiesemann, *Fully differential NNLO computations with MATRIX*, *Eur. Phys. J. C* **78** (2018) 537 [arXiv:1711.06631] [INSPIRE].

[6] S. Camarda et al., *DYTurbo: Fast predictions for Drell-Yan processes*, *Eur. Phys. J. C* **80** (2020) 251 [*Erratum ibid.* **80** (2020) 440] [arXiv:1910.07049] [INSPIRE].

[7] S. Catani et al., *Top-quark pair production at the LHC: Fully differential QCD predictions at NNLO*, *JHEP* **07** (2019) 100 [arXiv:1906.06535] [INSPIRE].

[8] J. Campbell and T. Neumann, *Precision Phenomenology with MCFM*, *JHEP* **12** (2019) 034 [arXiv:1909.09117] [INSPIRE].

[9] J.M. Campbell, R.K. Ellis and S. Seth, *Non-local slicing approaches for NNLO QCD in MCFM*, *JHEP* **06** (2022) 002 [arXiv:2202.07738] [INSPIRE].

[10] K. Fabricius, I. Schmitt, G. Kramer and G. Schierholz, *Higher Order Perturbative QCD Calculation of Jet Cross-Sections in e^+e^- Annihilation*, *Z. Phys. C* **11** (1981) 315 [INSPIRE].

[11] G. Kramer and B. Lampe, *Jet Cross-Sections in e^+e^- Annihilation*, *Fortsch. Phys.* **37** (1989) 161 [INSPIRE].

[12] W.T. Giele and E.W.N. Glover, *Higher order corrections to jet cross-sections in e^+e^- annihilation*, *Phys. Rev. D* **46** (1992) 1980 [INSPIRE].

[13] W.T. Giele, E.W.N. Glover and D.A. Kosower, *Higher order corrections to jet cross-sections in hadron colliders*, *Nucl. Phys. B* **403** (1993) 633 [hep-ph/9302225] [INSPIRE].

[14] S. Catani and M. Grazzini, *An NNLO subtraction formalism in hadron collisions and its application to Higgs boson production at the LHC*, *Phys. Rev. Lett.* **98** (2007) 222002 [hep-ph/0703012] [INSPIRE].

[15] I.W. Stewart, F.J. Tackmann and W.J. Waalewijn, *N-Jettiness: An Inclusive Event Shape to Veto Jets*, *Phys. Rev. Lett.* **105** (2010) 092002 [arXiv:1004.2489] [INSPIRE].

[16] M. Grazzini, *NNLO predictions for the Higgs boson signal in the $H \to WW \to l\nu l\nu$ and $H \to ZZ \to 4l$ decay channels*, *JHEP* **02** (2008) 043 [arXiv:0801.3232] [INSPIRE].

[17] S. Catani et al., *Vector boson production at hadron colliders: a fully exclusive QCD calculation at NNLO*, *Phys. Rev. Lett.* **103** (2009) 082001 [arXiv:0903.2120] [INSPIRE].

[18] G. Ferrera, M. Grazzini and F. Tramontano, *Associated WH production at hadron colliders: a fully exclusive QCD calculation at NNLO*, *Phys. Rev. Lett.* **107** (2011) 152003 [arXiv:1107.1164] [INSPIRE].

JHEP12(2023)193

[19] G. Ferrera, M. Grazzini and F. Tramontano, *Associated ZH production at hadron colliders: the fully differential NNLO QCD calculation*, *Phys. Lett. B* **740** (2015) 51 [arXiv:1407.4747] [INSPIRE].

[20] G. Ferrera, G. Somogyi and F. Tramontano, *Associated production of a Higgs boson decaying into bottom quarks at the LHC in full NNLO QCD*, *Phys. Lett. B* **780** (2018) 346 [arXiv:1705.10304] [INSPIRE].

[21] D. de Florian et al., *Differential Higgs Boson Pair Production at Next-to-Next-to-Leading Order in QCD*, *JHEP* **09** (2016) 151 [arXiv:1606.09519] [INSPIRE].

[22] S. Catani et al., *Diphoton production at hadron colliders: a fully-differential QCD calculation at NNLO*, *Phys. Rev. Lett.* **108** (2012) 072001 [*Erratum ibid.* **117** (2016) 089901] [arXiv:1110.2375] [INSPIRE].

[23] M. Grazzini, S. Kallweit, D. Rathlev and A. Torre, *$Z\gamma$ production at hadron colliders in NNLO QCD*, *Phys. Lett. B* **731** (2014) 204 [arXiv:1309.7000] [INSPIRE].

[24] M. Grazzini, S. Kallweit and D. Rathlev, *$W\gamma$ and $Z\gamma$ production at the LHC in NNLO QCD*, *JHEP* **07** (2015) 085 [arXiv:1504.01330] [INSPIRE].

[25] F. Cascioli et al., *ZZ production at hadron colliders in NNLO QCD*, *Phys. Lett. B* **735** (2014) 311 [arXiv:1405.2219] [INSPIRE].

[26] M. Grazzini, S. Kallweit and D. Rathlev, *ZZ production at the LHC: fiducial cross sections and distributions in NNLO QCD*, *Phys. Lett. B* **750** (2015) 407 [arXiv:1507.06257] [INSPIRE].

[27] T. Gehrmann et al., *W^+W^- Production at Hadron Colliders in Next to Next to Leading Order QCD*, *Phys. Rev. Lett.* **113** (2014) 212001 [arXiv:1408.5243] [INSPIRE].

[28] M. Grazzini et al., *W^+W^- production at the LHC: fiducial cross sections and distributions in NNLO QCD*, *JHEP* **08** (2016) 140 [arXiv:1605.02716] [INSPIRE].

[29] M. Grazzini, S. Kallweit, D. Rathlev and M. Wiesemann, *$W^\pm Z$ production at hadron colliders in NNLO QCD*, *Phys. Lett. B* **761** (2016) 179 [arXiv:1604.08576] [INSPIRE].

[30] M. Grazzini, S. Kallweit, D. Rathlev and M. Wiesemann, *$W^\pm Z$ production at the LHC: fiducial cross sections and distributions in NNLO QCD*, *JHEP* **05** (2017) 139 [arXiv:1703.09065] [INSPIRE].

[31] J. Gaunt, M. Stahlhofen, F.J. Tackmann and J.R. Walsh, *N-jettiness Subtractions for NNLO QCD Calculations*, *JHEP* **09** (2015) 058 [arXiv:1505.04794] [INSPIRE].

[32] R. Boughezal et al., *Color singlet production at NNLO in MCFM*, *Eur. Phys. J. C* **77** (2017) 7 [arXiv:1605.08011] [INSPIRE].

[33] J.M. Campbell, R.K. Ellis, Y. Li and C. Williams, *Predictions for diphoton production at the LHC through NNLO in QCD*, *JHEP* **07** (2016) 148 [arXiv:1603.02663] [INSPIRE].

[34] G. Heinrich et al., *NNLO predictions for Z-boson pair production at the LHC*, *JHEP* **03** (2018) 142 [arXiv:1710.06294] [INSPIRE].

[35] J.M. Campbell, T. Neumann and C. Williams, *$Z\gamma$ Production at NNLO Including Anomalous Couplings*, *JHEP* **11** (2017) 150 [arXiv:1708.02925] [INSPIRE].

[36] S. Catani et al., *Diphoton production at the LHC: a QCD study up to NNLO*, *JHEP* **04** (2018) 142 [arXiv:1802.02095] [INSPIRE].

[37] S. Abreu et al., *Quark and gluon two-loop beam functions for leading-jet p_T and slicing at NNLO*, *JHEP* **04** (2023) 127 [arXiv:2207.07037] [INSPIRE].

JHEP12(2023)193

[38] R. Boughezal, C. Focke, X. Liu and F. Petriello, *W-boson production in association with a jet at next-to-next-to-leading order in perturbative QCD*, *Phys. Rev. Lett.* **115** (2015) 062002 [arXiv:1504.02131] [INSPIRE].

[39] R. Boughezal et al., *Higgs boson production in association with a jet at NNLO using jettiness subtraction*, *Phys. Lett. B* **748** (2015) 5 [arXiv:1505.03893] [INSPIRE].

[40] R. Boughezal et al., *Z-boson production in association with a jet at next-to-next-to-leading order in perturbative QCD*, *Phys. Rev. Lett.* **116** (2016) 152001 [arXiv:1512.01291] [INSPIRE].

[41] R. Boughezal, X. Liu and F. Petriello, *W-boson plus jet differential distributions at NNLO in QCD*, *Phys. Rev. D* **94** (2016) 113009 [arXiv:1602.06965] [INSPIRE].

[42] S. Catani et al., *Top-quark pair hadroproduction at next-to-next-to-leading order in QCD*, *Phys. Rev. D* **99** (2019) 051501 [arXiv:1901.04005] [INSPIRE].

[43] S. Catani et al., *Bottom-quark production at hadron colliders: fully differential predictions in NNLO QCD*, *JHEP* **03** (2021) 029 [arXiv:2010.11906] [INSPIRE].

[44] S. Catani et al., *Higgs Boson Production in Association with a Top-Antitop Quark Pair in Next-to-Next-to-Leading Order QCD*, *Phys. Rev. Lett.* **130** (2023) 111902 [arXiv:2210.07846] [INSPIRE].

[45] L. Buonocore et al., *Associated production of a W boson and massive bottom quarks at next-to-next-to-leading order in QCD*, *Phys. Rev. D* **107** (2023) 074032 [arXiv:2212.04954] [INSPIRE].

[46] L. Buonocore et al., *Precise Predictions for the Associated Production of a W Boson with a Top-Antitop Quark Pair at the LHC*, *Phys. Rev. Lett.* **131** (2023) 231901 [arXiv:2306.16311] [INSPIRE].

[47] L. Cieri et al., *Higgs boson production at the LHC using the q_T subtraction formalism at N^3LO QCD*, *JHEP* **02** (2019) 096 [arXiv:1807.11501] [INSPIRE].

[48] S. Camarda, L. Cieri and G. Ferrera, *Drell-Yan lepton-pair production: qT resummation at N3LL accuracy and fiducial cross sections at N3LO*, *Phys. Rev. D* **104** (2021) L111503 [arXiv:2103.04974] [INSPIRE].

[49] G. Billis et al., *Higgs p_T Spectrum and Total Cross Section with Fiducial Cuts at Third Resummed and Fixed Order in QCD*, *Phys. Rev. Lett.* **127** (2021) 072001 [arXiv:2102.08039] [INSPIRE].

[50] X. Chen et al., *Third-Order Fiducial Predictions for Drell-Yan Production at the LHC*, *Phys. Rev. Lett.* **128** (2022) 252001 [arXiv:2203.01565] [INSPIRE].

[51] T. Neumann and J. Campbell, *Fiducial Drell-Yan production at the LHC improved by transverse-momentum resummation at N4LLp+N3LO*, *Phys. Rev. D* **107** (2023) L011506 [arXiv:2207.07056] [INSPIRE].

[52] X. Chen et al., *Transverse mass distribution and charge asymmetry in W boson production to third order in QCD*, *Phys. Lett. B* **840** (2023) 137876 [arXiv:2205.11426] [INSPIRE].

[53] S. Alioli et al., *Matching Fully Differential NNLO Calculations and Parton Showers*, *JHEP* **06** (2014) 089 [arXiv:1311.0286] [INSPIRE].

[54] S. Höche, Y. Li and S. Prestel, *Higgs-boson production through gluon fusion at NNLO QCD with parton showers*, *Phys. Rev. D* **90** (2014) 054011 [arXiv:1407.3773] [INSPIRE].

[55] P.F. Monni et al., *MiNNLO$_{PS}$: a new method to match NNLO QCD to parton showers*, *JHEP* **05** (2020) 143 [*Erratum ibid.* **02** (2022) 031] [arXiv:1908.06987] [INSPIRE].

JHEP12(2023)193

[56] J. Mazzitelli et al., *Next-to-Next-to-Leading Order Event Generation for Top-Quark Pair Production*, *Phys. Rev. Lett.* **127** (2021) 062001 [arXiv:2012.14267] [INSPIRE].

[57] S. Alioli et al., *Matching NNLO predictions to parton showers using N3LL color-singlet transverse momentum resummation in geneva*, *Phys. Rev. D* **104** (2021) 094020 [arXiv:2102.08390] [INSPIRE].

[58] A. Banfi, G.P. Salam and G. Zanderighi, *Resummed event shapes at hadron-hadron colliders*, *JHEP* **08** (2004) 062 [hep-ph/0407287] [INSPIRE].

[59] A. Banfi, G.P. Salam and G. Zanderighi, *Phenomenology of event shapes at hadron colliders*, *JHEP* **06** (2010) 038 [arXiv:1001.4082] [INSPIRE].

[60] S. Catani and M.H. Seymour, *The dipole formalism for the calculation of QCD jet cross-sections at next-to-leading order*, *Phys. Lett. B* **378** (1996) 287 [hep-ph/9602277] [INSPIRE].

[61] S. Catani and M.H. Seymour, *A general algorithm for calculating jet cross-sections in NLO QCD*, *Nucl. Phys. B* **485** (1997) 291 [hep-ph/9605323] [INSPIRE].

[62] S. Catani, S. Dittmaier, M.H. Seymour and Z. Trocsanyi, *The dipole formalism for next-to-leading order QCD calculations with massive partons*, *Nucl. Phys. B* **627** (2002) 189 [hep-ph/0201036] [INSPIRE].

[63] S. Frixione, Z. Kunszt and A. Signer, *Three jet cross-sections to next-to-leading order*, *Nucl. Phys. B* **467** (1996) 399 [hep-ph/9512328] [INSPIRE].

[64] S. Frixione, *A general approach to jet cross-sections in QCD*, *Nucl. Phys. B* **507** (1997) 295 [hep-ph/9706545] [INSPIRE].

[65] M. Dasgupta and G.P. Salam, *Resummation of nonglobal QCD observables*, *Phys. Lett. B* **512** (2001) 323 [hep-ph/0104277] [INSPIRE].

[66] C.W. Bauer, S. Fleming, D. Pirjol and I.W. Stewart, *An effective field theory for collinear and soft gluons: Heavy to light decays*, *Phys. Rev. D* **63** (2001) 114020 [hep-ph/0011336] [INSPIRE].

[67] C.W. Bauer, D. Pirjol and I.W. Stewart, *Soft collinear factorization in effective field theory*, *Phys. Rev. D* **65** (2002) 054022 [hep-ph/0109045] [INSPIRE].

[68] C.W. Bauer et al., *Hard scattering factorization from effective field theory*, *Phys. Rev. D* **66** (2002) 014017 [hep-ph/0202088] [INSPIRE].

[69] M. Beneke, A.P. Chapovsky, M. Diehl and T. Feldmann, *Soft collinear effective theory and heavy to light currents beyond leading power*, *Nucl. Phys. B* **643** (2002) 431 [hep-ph/0206152] [INSPIRE].

[70] M. Beneke and T. Feldmann, *Multipole expanded soft collinear effective theory with nonAbelian gauge symmetry*, *Phys. Lett. B* **553** (2003) 267 [hep-ph/0211358] [INSPIRE].

[71] L. Buonocore et al., *Effective transverse momentum in multiple jet production at hadron colliders*, *Phys. Rev. D* **106** (2022) 014008 [arXiv:2201.11519] [INSPIRE].

[72] J.C. Collins and F.V. Tkachov, *Breakdown of dimensional regularization in the Sudakov problem*, *Phys. Lett. B* **294** (1992) 403 [hep-ph/9208209] [INSPIRE].

[73] M. Beneke, *Lectures on "Soft-Collinear Effective Theory"*, in proceedings of the *Helmholtz International Summer School on Heavy Quark Physics* Moscow, Dubna, Russian Federation, June 9–10 (2005).

[74] J. Collins, *Foundations of perturbative QCD*, Cambridge University Press (2013) [DOI:10.1017/9781009401845].

JHEP12(2023)193

[75] M. Beneke and V.A. Smirnov, *Asymptotic expansion of Feynman integrals near threshold*, *Nucl. Phys. B* **522** (1998) 321 [hep-ph/9711391] [INSPIRE].

[76] V.A. Smirnov, *Applied asymptotic expansions in momenta and masses*, *Springer Tracts Mod. Phys.* **177** (2002) 1 [INSPIRE].

[77] A. Mukherjee and W. Vogelsang, *Jet production in (un)polarized pp collisions: dependence on jet algorithm*, *Phys. Rev. D* **86** (2012) 094009 [*Erratum ibid.* **107** (2023) 119901] [arXiv:1209.1785] [INSPIRE].

[78] S. Catani, M. Grazzini and A. Torre, *Transverse-momentum resummation for heavy-quark hadroproduction*, *Nucl. Phys. B* **890** (2014) 518 [arXiv:1408.4564] [INSPIRE].

[79] L. Buonocore, M. Grazzini, J. Haag and L. Rottoli, *Transverse-momentum resummation for boson plus jet production at hadron colliders*, *Eur. Phys. J. C* **82** (2022) 27 [arXiv:2110.06913] [INSPIRE].

[80] S. Catani, S. Devoto, M. Grazzini and J. Mazzitelli, *Soft-parton contributions to heavy-quark production at low transverse momentum*, *JHEP* **04** (2023) 144 [arXiv:2301.11786] [INSPIRE].

[81] D. Bertolini et al., *Soft Functions for Generic Jet Algorithms and Observables at Hadron Colliders*, *JHEP* **07** (2017) 099 [arXiv:1704.08262] [INSPIRE].

[82] Z. Kunszt, A. Signer and Z. Trocsanyi, *Singular terms of helicity amplitudes at one loop in QCD and the soft limit of the cross-sections of multiparton processes*, *Nucl. Phys. B* **420** (1994) 550 [hep-ph/9401294] [INSPIRE].

[83] Y.-T. Chien et al., *Recoil-free azimuthal angle for precision boson-jet correlation*, *Phys. Lett. B* **815** (2021) 136124 [arXiv:2005.12279] [INSPIRE].

[84] S. Catani, Y.L. Dokshitzer, M.H. Seymour and B.R. Webber, *Longitudinally invariant K_t clustering algorithms for hadron hadron collisions*, *Nucl. Phys. B* **406** (1993) 187 [INSPIRE].

[85] S.D. Ellis and D.E. Soper, *Successive combination jet algorithm for hadron collisions*, *Phys. Rev. D* **48** (1993) 3160 [hep-ph/9305266] [INSPIRE].

[86] J.C. Collins, D.E. Soper and G.F. Sterman, *Transverse Momentum Distribution in Drell-Yan Pair and W and Z Boson Production*, *Nucl. Phys. B* **250** (1985) 199 [INSPIRE].

[87] J. Butterworth et al., *PDF4LHC recommendations for LHC Run II*, *J. Phys. G* **43** (2016) 023001 [arXiv:1510.03865] [INSPIRE].

[88] A. Buckley et al., *LHAPDF6: parton density access in the LHC precision era*, *Eur. Phys. J. C* **75** (2015) 132 [arXiv:1412.7420] [INSPIRE].

[89] M. Cacciari, G.P. Salam and G. Soyez, *The anti-k_t jet clustering algorithm*, *JHEP* **04** (2008) 063 [arXiv:0802.1189] [INSPIRE].

[90] F. Cascioli, P. Maierhöfer and S. Pozzorini, *Scattering Amplitudes with Open Loops*, *Phys. Rev. Lett.* **108** (2012) 111601 [arXiv:1111.5206] [INSPIRE].

[91] F. Buccioni, S. Pozzorini and M. Zoller, *On-the-fly reduction of open loops*, *Eur. Phys. J. C* **78** (2018) 70 [arXiv:1710.11452] [INSPIRE].

[92] F. Buccioni et al., *OpenLoops 2*, *Eur. Phys. J. C* **79** (2019) 866 [arXiv:1907.13071] [INSPIRE].

[93] S. Actis et al., *RECOLA: REcursive Computation of One-Loop Amplitudes*, *Comput. Phys. Commun.* **214** (2017) 140 [arXiv:1605.01090] [INSPIRE].

[94] A. Denner, J.-N. Lang and S. Uccirati, *Recola2: REcursive Computation of One-Loop Amplitudes 2*, *Comput. Phys. Commun.* **224** (2018) 346 [arXiv:1711.07388] [INSPIRE].

JHEP12(2023)193

[95] A. Denner, S. Dittmaier and L. Hofer, *Collier: a fortran-based Complex One-Loop LIbrary in Extended Regularizations*, *Comput. Phys. Commun.* **212** (2017) 220 [arXiv:1604.06792] [INSPIRE].

[96] S. Catani and B.R. Webber, *Infrared safe but infinite: Soft gluon divergences inside the physical region*, *JHEP* **10** (1997) 005 [hep-ph/9710333] [INSPIRE].

[97] NNPDF collaboration, *Parton distributions from high-precision collider data*, *Eur. Phys. J. C* **77** (2017) 663 [arXiv:1706.00428] [INSPIRE].

[98] S. Catani and M. Grazzini, *QCD transverse-momentum resummation in gluon fusion processes*, *Nucl. Phys. B* **845** (2011) 297 [arXiv:1011.3918] [INSPIRE].

[99] X.-D. Ji, J.-P. Ma and F. Yuan, *QCD factorization for semi-inclusive deep-inelastic scattering at low transverse momentum*, *Phys. Rev. D* **71** (2005) 034005 [hep-ph/0404183] [INSPIRE].

[100] J.-Y. Chiu et al., *Soft-Collinear Factorization and Zero-Bin Subtractions*, *Phys. Rev. D* **79** (2009) 053007 [arXiv:0901.1332] [INSPIRE].

[101] T. Becher and G. Bell, *Analytic Regularization in Soft-Collinear Effective Theory*, *Phys. Lett. B* **713** (2012) 41 [arXiv:1112.3907] [INSPIRE].

[102] J.-Y. Chiu, A. Jain, D. Neill and I.Z. Rothstein, *A formalism for the Systematic Treatment of Rapidity Logarithms in Quantum Field Theory*, *JHEP* **05** (2012) 084 [arXiv:1202.0814] [INSPIRE].

[103] M.G. Echevarria, I. Scimemi and A. Vladimirov, *Universal transverse momentum dependent soft function at NNLO*, *Phys. Rev. D* **93** (2016) 054004 [arXiv:1511.05590] [INSPIRE].

[104] Y. Li, D. Neill and H.X. Zhu, *An exponential regulator for rapidity divergences*, *Nucl. Phys. B* **960** (2020) 115193 [arXiv:1604.00392] [INSPIRE].

[105] J. Chay and C. Kim, *Consistent treatment of rapidity divergence in soft-collinear effective theory*, *JHEP* **03** (2021) 300 [arXiv:2008.00617] [INSPIRE].

[106] S. Catani and P.K. Dhani, *Collinear functions for QCD resummations*, *JHEP* **03** (2023) 200 [arXiv:2208.05840] [INSPIRE].

[107] C.W. Bauer, A.V. Manohar and P.F. Monni, *Disentangling observable dependence in $SCET_I$ and $SCET_{II}$ anomalous dimensions: angularities at two loops*, *JHEP* **07** (2021) 214 [arXiv:2012.09213] [INSPIRE].

JHEP12(2023)193